ASIA-PACIFIC NETWORK FOR
GLOBAL CHANGE RESEARCH

Project Reference Number: ARCP2013-12CMY-Burnett

Assessing the Impact of Climate Change and Development Pressures on Nutrient Inputs into the Mekong River and Tonle Sap

The following collaborators worked on this project:

1. William C. Burnett (Project Leader), Florida State University, wburnett@fsu.edu

2. Gullaya Wattayakorn, Chulalongkorn University (Thailand), gullaya@chula.ac.th

3. Veasna Kum, Ministry of Environment (Cambodia), veasna_kum@yahoo.com

4. Khamfeuane Sioudom, National University of Laos, khamfeuane@fe-nuol.edu.la

Project Reference Number: ARCP2013-12CMY-Burnett

Assessing the Impact of Climate Change and Development Pressures on Nutrient Inputs into the Mekong River and Tonle Sap

Final Report Submitted to APN

Page Left Intentionally Blank

Part One: Overview of Project Work and Outcomes

Non Technical Summary

We have investigated the relationships between Mekong River/Tonle Sap hydrology, the dissolved and particulate phosphorus (P) cycle and aquatic productivity (measured via chlorophyll-a) in the Tonle Sap/Mekong River system. This involved measurements in the contiguous Mekong Region countries Thailand, Laos, and Cambodia. Emphasis was place on Tonle Sap Lake, the largest and most productive lake in SE Asia. We hypothesized that P is the limiting nutrient in this system, and feel that its sources and transformations have not previously been well described. We further hypothesized that the P cycle is intimately related to the hydrologic cycle of this flood pulse system. Geochemical measurements and modelling were used to determine the sources of P to the lake and its relationship to the hydrologic stage of the river and lake. We were particularly interested in evaluating the role of groundwater to the P cycle, an area that has been largely ignored. Our approach consisted of combining continuous measurements of radon, a groundwater tracer, with detailed P speciation measurements. The overarching objectives were to assess and model nutrient and productivity impacts in response to climate change, dam construction or other development activities in the Mekong River basin that will affect downstream river flow.

Keywords

Mekong River, Tonle Sap Lake, phosphorus, radon, groundwater

Objectives

This project was designed to meet the following objectives: (i) Establish the temporal and spatial patterns of phosphorus species in the Mekong River, Tonle Sap River and Tonle Sap Lake and determine the major nutrient sources. (ii) Measure key environmental parameters with special attention to those that may influence P concentration/speciation (O_2, temperature, conductivity, total suspended sediments) as well as those parameters that are needed to assess nutrient limitation. (iii) Develop a system dynamics (SD) model that will relate biologically available P concentrations to the hydrologic cycle of the lake. (iv) Develop a mass balance model to evaluate groundwater and dissolved P inflow to the lake at different stages of the hydrological cycle. (v) Broader aspect objectives included training and capacity building of scientists and students in Laos, Thailand and Cambodia. This was accomplished mainly through hands-on research experience of students in the field.

Amount Received and Number of Years Supported

The Grant awarded to this project was:

US$ 41,000 for Year 1:

US$ 27,100 for Year 2:

Activities Undertaken

The following summarizes the activities and milestones of our project:

a. Sampling of the Mekong River in July 2012 (self-funded) on the Thailand side of the river between Nong Khai and Mukdahan
b. Meeting with Mekong River Commission (MRC) officials in Vientiane concerning overlapping interests and access to their water quality measurements in Oct 2012
c. Mekong River sampling in Laos between Pakse and the Cambodian border in Oct 2012
d. Meeting with START personnel in Bangkok; posting of project summary on their web page
e. Non-commercial license received from MRC allowing access to MRC water quality data base
f. Detailed survey and sampling of Tonle Sap Lake in January 2013, July 2013, June 2014, and November 2014
g. Detailed sampling and surveying of the Tonle Sap and Mekong Rivers in September 2013
h. Meeting of Principal Investigators and presentations to faculty, students of Chulalongkorn University and START personnel; Bangkok, February 2015

Results

A radon mass balance model based on data collected during this project indicates that the groundwater flow to Tonle Sap Lake is about 10.3 km^3/yr. This is about half the flow from all the tributaries that enter the lake. In spite of the lower flow, groundwater contributes about the same amount of phosphorus as the tributaries because of the higher phosphorus concentrations in groundwater. While much of this groundwater is likely re-circulated lake water ('bank storage'), it is still important as a nutrient contributor. As lake water penetrates the subsurface, nutrients will be released from the solid phases of the shallow aquifer by organic matter decomposition and other processes. In addition, some upland groundwater will contribute to this total and add some amount of 'new' nutrients to the lake. Our results suggest that the groundwater contribution of the most biologically important species of phosphorus, dissolved inorganic phosphorus, is about 30% of all the estimated inflows including the Tonle Sap River, tributaries and sediments as well as groundwater. Results for sediments indicated that resuspension could supply nearly as much as groundwater while diffusion of DIP from sediments is minor compared to the other sources. Inputs from sewage, fertilizers, and other human sources have not been determined.

Relevance to the APN Goals, Science Agenda and to Policy Processes

Goals: Outputs of our project can be used by national policy makers and the Mekong River Commission (MRC) to assess potential effects on nutrient budgets caused by changes in Mekong River flow.

Science Agenda: Our research has provided a new methodology for assessing the effects on nutrient budgets caused by changes in river flow, whether from development (e.g., dams), climate change, or a combination of both.

Policy Processes: Many policy decisions will need to be made over the coming years concerning Mekong Basin development (e.g., the Xayaburi dam in northern Laos and many others proposed). This project has provided a model to assess the effects on nutrient inflows to Tonle Sap Lake as well as extension to other lower Mekong River areas.

Self-evaluation

In general, things went well with the project. The component that proved to be most troublesome was the monthly time series. The costs turned out to be higher than expected and the logistics even more difficult. We did manage to combine efforts with the MRC contract lab in Phnom Penh. They collected and analysed samples from Kampong Loung on the permanent lake every month. We also did some mining of the historical MRC water quality data. Unfortunately, that data set is not updated on a regular basis.

Overall, we think the project has made good progress with a limited budget and amount of time.

Potential for further work

We have limited this study to an investigation of natural sources of nutrients. However, with increased development in the basin, anthropogenic sources will likely become increasingly more important. Sewage inputs to the lake and use of fertilizers will likely increase in the years ahead. Quantifying these types of nutrient inputs and analysing how they may be affected by changes in the hydrologic cycle should be investigated.

Publications

Kum, V. and W.C. Burnett, 2013. Modeling phosphorus dynamics of Tonle Sap Lake. International Journal of Environment and Resource, 2, 14-23.

Burnett, W.C., Wattayakorn, G., Kum, V., and Sioudom, K., 2013. Nutrient sources to Tonle Sap Lake, Cambodia. APN Science Bulletin, 3, 108-112.

Burnett, W.C., Wattayakorn, G., Kum, V., and Sioudom, K., 2014. Phosphorus dynamics in Tonle Sap Lake, Cambodia. APN Science Bulletin, 4, 85-88.

Chanyotha, S., C. Kranrod, and W.C. Burnett, 2014. Assessing diffusive fluxes and pore water radon activities via a single automated experiment. Journal of Radioanalytical and Nuclear Chemistry, 301, 581-588.

References

A complete reference list may be found at the end of Part 2 (Technical Report).

Acknowledgments

We have many people to thank for their cooperation and assistance during this project. Bunseang Suy (Tonle Sap Rural Water Supply, Battambang, Cambodia) was extremely helpful in arranging many of the logistics for our field studies. Dr. Matti Kummu (Water and Development Research Group, Aalto University, Finland) was kind enough to provide us with his data on lake water levels, river discharge values, etc., which greatly assisted our modelling efforts. Ms. Sophea Nhim (Ministry of Water Resource and Meteorology, Phnom Penh) supervised the sampling and analysis of the samples from the one-year time series. Dr. Jariya Boonjawat (START and Chulalongkorn University) allowed us to post project plans on the START website. Finally, we thank the following for their very capable assistance in the field: Dr. Supitcha Chanyotha, Ratsirin "Prae" Supcharoen, Rawiwan "O" Kritsananuwat, Pongjit "Tarn" Jaiboon (all from Chulalongkorn University), Butsawan "Nok" Bidorn (Florida State University), and Dalasack Xayyasouk (National University of Laos).

Part Two: Technical Report

Preface

This report contains a detailed account of our two-year APN study of nutrient sources into Tonle Sap Lake. We present below the first attempt to quantify all natural sources of phosphorus (P) to the lake and show how P is distributed between the following fractions: total phosphorus (TP), total dissolved P (TDP), dissolved inorganic P (DIP), dissolved organic P (DOP), and particulate P (PP). We showed that the main sources of DIP, the most biologically available form, to the lake are from the tributaries and groundwater. Additional sources include the Tonle Sap River, resuspension of sediments, and diffusion from sediments. Our nutrient data are consistent with the concept that the primary productivity in the lake is P-limited.

Table of Contents

1. Introduction

The Flood Pulse Concept

Floods are the primary drivers in determining the structure and function of tropical, lowland river-floodplain ecosystems, as encapsulated by the “Flood Pulse Concept” presented originally by Junk et al. (1989). This concept highlights the importance of lateral connections in the functioning of river-floodplain systems. Regularity is central to the importance of the flood pulse in tropical systems, allowing biota to evolve adaptations that enable exploitation of newly accessible habitat and the ‘pulse’ in nutrient availability and primary productivity associated with floodplain inundation. The pulse is thus seen to stimulate a chain-reaction of increased productivity, which is transferred up the food chain. Junk et al. (1999) observed that periodic floodplain inundation increases the availability of nutrients and rates of organic matter recycling, increasing the potential for primary and hence secondary production. The floodplain is thus able to support an increased biomass and diversity of biota, which have adapted to exploit this periodically available habitat and resource, producing a characteristic community structure.

Evidence accumulated from a number of controlled laboratory experiments suggests that re-flooding of dried wetland sediments can result in a significant release of both nitrogen and phosphorus into the water column (Briggs et al., 1985; Fabre, 1988; Qiu and McComb, 1994, 1996; Turner and Haygarth, 2001). However, these findings have been contradicted by numerous other laboratory studies where no significant release of nutrients into the water column occurred following re-flooding (Qiu and McComb, 1994; Mitchell and Baldwin, 1998; Mitchell and Baldwin, 1999; Baldwin et al., 2000).

The Role of Groundwater

Thus, while there is evidence that in at least some cases floodplain inundation results in nutrient release, the controlling mechanisms are not clear. In addition, no serious consideration has been given to groundwater as a nutrient source in a flood pulse system. One of the main themes of our project has been to examine *the role of groundwater* as a nutrient pathway within Tonle Sap Lake, a classic flood-pulse setting. We have focused our attention on phosphorus (P), as it is has often been identified as the limiting nutrient in many freshwater systems (Schindler, 1970, 1978; Hecky and Kilham, 1988; Søballe and Kimmel, 1987; Baines and Pace, 1994). More recently, however, it has been argued that co-limitation by other nutrients in concert with P may be common in lacustrine systems (Sterner 2008; Elser et al. 2007). While the flood pulse concept has received a lot of attention, little consideration has been paid specifically to P biogeochemistry and how groundwater may be a significant driver within this context. One of our primary objectives was thus to examine the P cycle and its relationship to the unusual surface hydrology of Tonle Sap Lake, an excellent example of a flood pulse system.

Tonle Sap Lake

Tonle Sap, the largest freshwater lake in SE Asia (**Fig. 1**), hosts one of the most productive inland fisheries in the world, accounting for more than 75% of Cambodia’s inland fish catch and ~60% of the country's protein needs (Lamberts, 2006). Because there have been relatively few scientific studies, details are lacking concerning the mechanisms that supply nutrients to maintain the high biological productivity that is characteristic of the lake. In addition, accelerating development of dams and diversion projects in the Lower Mekong Basin now pose unknown threats to the lake’s hydrologic cycle and ecosystem.

During the dry season (October to May) water from the lake flows south through a tributary (Tonle Sap River) and discharges to the Mekong River near Phnom Penh. This flow is significant, representing about 50% of the discharge to the Mekong Delta, Vietnam. By the end of the dry season, the lake reaches its lowest level, with an average depth of less than 1 m (**Table 1**). When the monsoon rains begin again (usually May or June), the Mekong River flow increases dramatically, forcing a reversal of flow direction in the connecting tributary, resulting in addition of huge volumes of water back into the lake. The result is a ~6-fold increase in lake surface area, a water depth approaching 10 m, and a net change in volume from ~1.6 km^3 (dry season) to 60-80 km^3 (wet season) depending upon the intensity of the flood each year (Sarkkula et al., 2003). While the flood pattern varies somewhat from year-to-year, it is remarkably consistent (**Fig. 2**). According to a recent study by Day et al. (2011), the transition from a non-pulsing lake to the Mekong-connected pulsing system found today occurred about 4,000 years ago. So this natural system has been operating for a very long time.

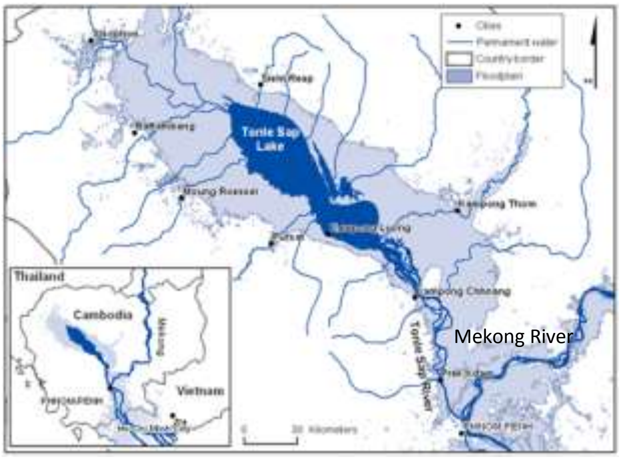

Fig. 1. Map of Tonle Sap Lake, showing the Mekong River, and their connection via the Tonle Sap River. Dark colour represents the permanent lake; lighter colour shows extent of floodplain.

Table 1. Average characteristics of Tonle Sap Lake at low water level and flood stage (Kummu et al., 2008).

Parameter	Low Water Level (Apr/May)	Flood Stage (Oct/Nov)
Area (km^2)	2,240	13,220
Length (km)	120	250
Width (km)	35	100
Volume (m^3)	1.6×10^9	59.6×10^9
Depth (m)*	0.5	7

*Average depths measured at low and high water level during our expeditions were 0.58 m and 6.7 m, respectively.

What are the nutrient sources that maintain the high productivity of Tonle Sap? The lake is thought to be P-limited, as are most fresh water systems, so the P cycle is of particular interest. N-fixation via cyanobacteria that populate the lake (especially during the dry season; Ohtaka et al., 2010) may drive the lake towards P limitation. Lamberts et al. (2007) suggested that P bound to suspended sediment brought in during the annual flood, and deposited on the lakebed, might be released by reductive dissolution of metal oxides.

The sources and mechanisms of nutrient supply to Tonle Sap, and how fluctuations in the supply and bioavailability of nutrients are related to the hydrologic cycle, and to groundwater inputs in particular, are not well understood. Identification of the mechanisms and processes that control P supply and bioavailability in this system will provide valuable insights that can be extrapolated to other flood-pulse systems worldwide. It is also important to recognize the linkages between the lake's unusual hydrologic cycle and nutrient inputs as upstream development may alter these annual cycles.

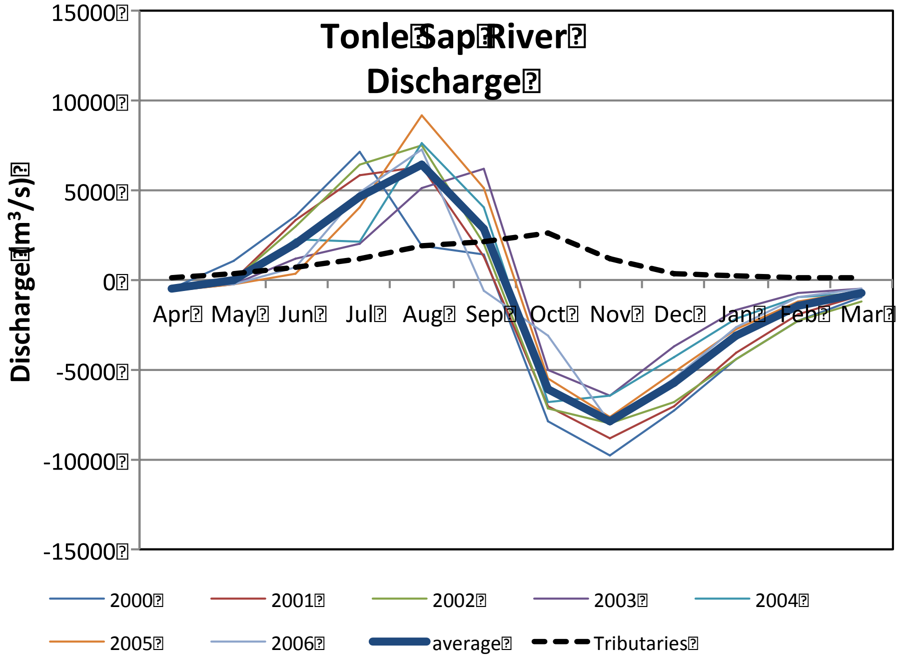

Fig. 2. Variations of discharge of the Tonle Sap River as well as the total discharge of all tributaries from 2000 through 2006. Positive values represent flow into TSL while negative values are for flows exiting the lake through the TSR. Data compiled by M. Kummu (pers. comm.).

Objectives

This project was designed to meet the following objectives: (i) establish the temporal and spatial patterns of P species in the Mekong River/Tonle Sap Lake system and determine the major nutrient sources. (ii) Measure key environmental parameters with special attention to those that may influence P concentration/speciation (O_2, temperature, conductivity, and suspended sediment concentrations) as well as those parameters that are needed to assess nutrient limitation (N and P species). (iii) Develop a system dynamics (SD) model that will relate biologically available P concentrations to the hydrologic cycle of the lake. (iv) Develop a mass balance model to evaluate groundwater and dissolved P inflow to the lake at different stages of the hydrological cycle. (v) Broader aspect objectives included training and capacity building of scientists and students in Laos, Thailand and Cambodia. This was accomplished mainly through hands-on research experience of graduate students in the field.

2. Methodology

Surveys

We conducted an initial survey in the Mekong River where it separates Thailand and Laos (July 2012) and another survey further downstream in Laos just before the Cambodian border (October 2012). An additional fieldtrip was conducted in the Tonle Sap River (TSR) and its confluence with the Mekong River in Cambodia (Sep. 2013). Four surveys were run in Tonle Sap Lake (TSL; Jan. and Jul., 2013; and Jun. and Nov., 2014). All lake surveys and the TSR survey included continuous measurements of radon and conductivity as groundwater tracers. During each survey, we stopped at approximately hourly intervals to collect samples for major nutrients (filtered and unfiltered), suspended sediment concentrations, and chlorophyll-a analysis (in total >130 stations were occupied).

Radon and Conductivity Measurements

Dissolved radon was analysed using the automated systems described in Burnett et al. (2001) and Dulaiova et al. (2005). Surveys were conducted from a boat with underway speeds of less than 5 km/hr to optimize spatial resolution. The multi-detector system used measures ^{222}Rn from a constant stream of water passing through an air-water exchanger that distributes radon between the water and a closed air loop. The enriched air is fed to three commercial radon-in-air monitors (RAD-7, Durridge Co.) arranged in parallel that measure the activity of ^{222}Rn via measurement of the short-lived ($T_{1/2}$ = 3 min) α-emitting daughter, ^{218}Po. Radon activity in water is then calculated from the temperature-dependent solubility coefficient (Weigel, 1978). Radon counts were integrated over either 5 or 10-minute cycles with resulting measurement uncertainties of 10-15%. Continuous temperature and electrical conductivity measurements were recorded with a Van Essen Instruments CTD Diver attached to the submersible pump used to deliver water to the air-water exchanger. These probes were calibrated to conductivity standards before each field excursion.

Groundwater samples were collected from about 40 'tube' wells in the northern portion of TSL during an earlier project. These wells were installed to a depth of 5-10m by various NGO's as a source of fresh water. Measurement of radon in groundwater samples was carried out in the field using a RAD-H_2O accessory that aerates a 250-mL water sample in a closed loop with the RAD-7. During a five-minute aeration, more than 95% of the available radon is removed from the water. Duplicate measurements indicated that the precision of this method is approximately 10%.

We also estimated dissolved radon activities in pore fluids (groundwater) by performing equilibrations with sediment samples collected from various points in TSL. These equilibrations consisted of adding known amounts of sediment and water in gas-tight vessels and running air through the sample flask and then to a radon monitor in a closed loop (Corbett et al. 1998; Chanyotha et al., 2014). Since groundwater flow rates are typically slow, on the order of cm/day, there should be sufficient time to reach equilibrium conditions for water flow through geologically similar materials. This approach, therefore, can offer a reasonable estimate of effective radon activities in discharging groundwaters.

Nutrient Analyses

River, lake and groundwater samples were collected in sample-rinsed polyethylene bottles, and filtered through HCl-washed Whatman GF/C filters immediately upon sample collection. Separate samples from each station (except the groundwater samples) were collected without filtering for "total" analysis. The samples were kept dark on ice and returned shortly after collection to the chemical laboratories at Chulalongkorn University for total nitrogen (TN) and phosphorus (TP), nitrate (NO_3, actually nitrate + nitrite), ammonia (NH_4), dissolved inorganic nitrogen (DIN, total of NO_3, NO_2 and NH_4), dissolved inorganic phosphorus (DIP), total dissolved phosphorus (TDP), dissolved organic phosphorus (DOP, the difference between TDP and DIP), and particulate phosphorus (PP, the difference between TP and TDP) following recommended procedures (Strickland and Parsons, 1972; Clesceri et al., 1998). Total dissolved N (TDN) and P (TDP) were analysed following the same chemical and spectrographic procedures but after persulfate oxidation. Chlorophyll-a concentrations were analysed by a spectrophotometric method, utilizing a 90% acetone extraction (Strickland and Parsons 1972; Sartory and Grobbelaar, 1984). Water samples for chlorophyll-a determinations were filtered through pre-washed Whatman GF/F filters as soon as possible after collection, and stored at -10°C before analysis within 2 weeks.

P-Release Experiments

A simple batch experiment was set up to investigate the release of phosphorus from suspended sediment during a simulated re-suspension event. Two bottom sediment samples, one from the north end (TS32) and one from the south end of the lake (TS60), were collected with an Ekman dredge. We collected the top layers from these sediment samples to be used in this laboratory study. Samples were put on ice during transport to the laboratory where they were stored at 4ºC until used in the experiments. Wet sediment was suspended in deionized water, in beakers, in each of the following concentrations: 100, 200, 300, 500, 1000, 1500 and 2000 mg/L. Re-suspension of the sediment was maintained by means of magnetic stir bars inside each of the beakers. Water samples were collected from each beaker at 0, 1, 2, 4, 6, and 8 hours following introduction of the sediment. Unfiltered samples were analyzed for TP, additional samples were collected and filtered through Whatman GF/C filters and analyzed for DIP and TDP.

3. MODELING APPROACHES

Systems Dynamic Modeling

System Dynamics (SD) modelling was developed in the 1960s by Jay Forrester who applied concepts from feedback control theory to the study of complex systems. SD has been applied to a wide range of fields including biology, ecology, engineering, medicine, public policy, business, economics, and psychology. SD is much less dependent on quantitative data than some alternative modelling methodologies. In SD, the conceptualization of feedback processes is more crucial than exact parameterization. Also, SD modelling predicts future states by showing feedback mechanisms among the system components rather than forecasting future states using time series data (Ford, 1999 and references therein). Thus, SD is especially appropriate for a study aiming at maximizing the utilization of geochemical and ecological data by incorporating qualitative (as well as quantitative) information so that a complex, imprecisely defined chemical/ecological system can be studied quantitatively, effectively, and comprehensively. These features and the way an SD model is conceptualized make this methodology particularly appropriate for this research because data for many variables needed for the analysis do not currently exist.

The P model we developed is a mathematical representation of the major stocks in the aquatic P cycle, and the in-river and lake processes that determine the transfer of P between those stocks. The model simulates the mean river flow, total dissolved phosphorus (TDP) concentrations (assumed here the most biologically available phosphorus) and total phosphorus (TP). The model also includes groundwater inputs that are related to the hydrologic cycle. The rates of mass transfer between reservoirs in the model were modelled as first-order linear exchanges. While the equations are composed of linear exchanges, the combined response is non-linear. We used a System Dynamics software (Vensim) to solve the linked differential equations. The SD model developed during this project was formulated for the Tonle Sap system and calibrated with the data collected by our measurements. See the appendix for a more complete explanation of the SD modelling.

Mass Balance Estimates of Groundwater Inputs

We have estimated groundwater discharge into TSL by a radon mass balance "flux by difference" approach (Charette et al., 2008). Radon (^{222}Rn, $T_{1/2}$ = 3.82 days) is a good tracer of groundwater flow because its concentration in groundwater is much greater than in surface waters, it is conservative, and can be measured continuously. We set up the mass balance (**Fig. 3**) as follows:

$F_{gw} = F_{riv} + F_{tri} + F_{dif} – F_{atm} – F_{decay} – F_{mix}$

where F_{gw} represents the radon flux via groundwater; F_{riv} is the radon flow in or out of the lake via the TSR; F_{tri} is inputs from tributaries; F_{dif} represents the addition of radon by diffusion from sediments; and F_{atm}, F_{decay} and F_{mix} are losses by atmospheric evasion, radioactive decay and mixing with low radon lake waters, respectively. Note that the F_{riv} term represents an addition of radon during the flood season (~June-September) while it is a loss during the dry season (~October-May) when the lake is draining through the TSR. All fluxes have been estimated on an average monthly basis with units of disintegrations per minute (dpm) per square meter per day (dpm/m^2 day).

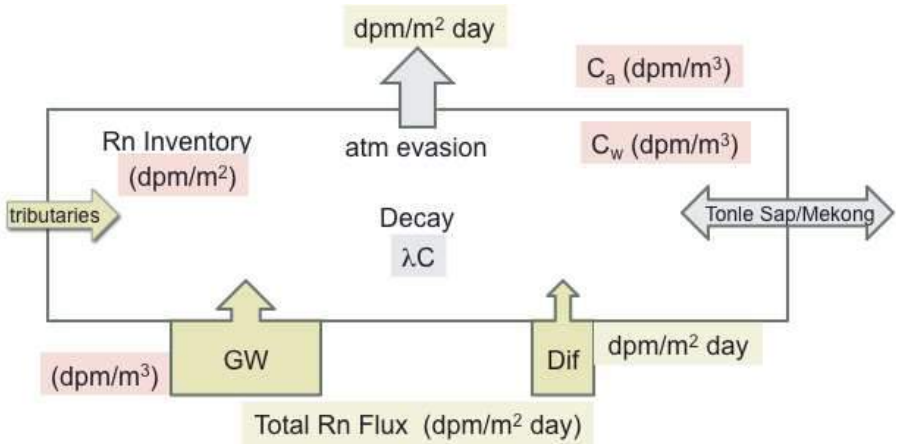

Fig. 3. Conceptual view of the radon mass balance. Inputs of radon to the lake from rivers, tributaries, groundwater and diffusion are balanced by loss to the atmosphere, export via the Tonle Sap River during the dry season, and radioactive decay.

The river and tributary inputs and outputs can be estimated by the following two equations:

$F_{riv} = [Q_{riv}\ (m^3/s) * C_{Rn}\ (dpm/m^3) * 86{,}400\ (s/day)]/A\ (m^2)$

$F_{tri} = [Q_{tri}\ (m^3/s) * C_{Rn}\ (dpm/m^3) * 86{,}400\ (s/day)]/A\ (m^2)$

where Q_{riv} and Q_{tri} represent the discharges of the TSR and all tributaries that connect with TSL; C_{Rn} is the activity concentration of radon in TSR and the tributaries; and A is the area of the lake. Average monthly values for Q (**Fig. 2**) and A (**Fig. 4**) were made available from Kummu et al. (2013) and Kummu (pers. comm.).

Inputs of radon to the lake from diffusion are calculated from an advection-diffusion equation as explained by Cable et al. (1996):

$$\frac{dC}{dt} = K_z \frac{\partial^2 C}{\partial z^2} + \omega \frac{\partial C}{\partial z} + P + \lambda C$$

where C is the radon activity concentration in wet sediment, t is time, z is depth in the sediment, *Kz* is the vertical diffusivity, ω is the vertical advective velocity (+ downwards), P is the production of radon from the ^{226}Ra in the sediment ($P = \lambda C_{eq}$; λ is the decay constant for $^{222}Rn = 0.181\ day^{-1}$), C_{eq} is the equilibrium activity of radon in the groundwater, and λC is the decay of radon. We also made several direct measurements of radon diffusion from TSL sediments experimentally in the laboratory (Chanyotha et al., 2014).

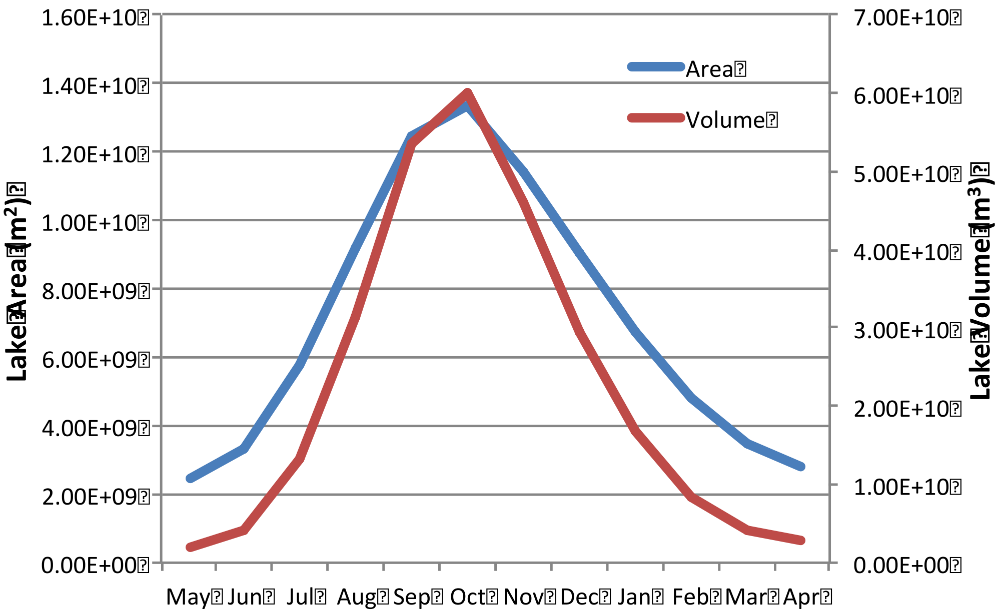

Fig. 4. Average variations of Tonle Sap Lake area and volume over the course of a hydrologic year. Averages calculated from data collected by M. Kummu from 2000 through 2006.

For atmospheric loss (F_{atm}) estimates, we used standard gas exchange formulations as summarized by MacIntyre et al. (1995). The basic equations are as follows:

$$F_{atm} = k\left(C_w - aC_{atm}\right)$$

$$k(600) = 0.45u_{10}^{1.6}(Sc/600)^{-0.5}$$

where k is the gas exchange coefficient or piston velocity; C_w and C_{atm} are the radon concentrations in the lake water and overlying atmosphere, respectively; μ_{10} is wind speed measured 10 meters above the ground; and S_c is the Schmidt number, the ratio of the kinematic viscosity (v) to the molecular diffusion coefficient (D_m). Wind speeds were recovered from weather stations in Siem Reap and Phnom Penh for the periods of our surveys.

Finally, decay and mixing losses are assessed by:

$F_{decay} = \lambda\ (1/day) * I\ (dpm/m^2)$

$F_{mix} = I/\tau$

Where I represents the inventory of radon in the lake waters and τ is the residence time of the lake (assumed to be 180 days; the approximate amount of time to replace the lake volume).

4. Results & Discussion

Radon and Conductivity Trends

We illustrate the radon/conductivity trends by showing some of the results from our July 14-18, 2013 fieldtrip to TSL (**Fig. 5**). Two main features are apparent; there are 'hotspots' of high radon near the boundary between the permanent lake and the floodplain. The other feature is the relatively low and fairly constant radon in the open lake. We encountered these high radon areas when we entered and exited the permanent lake through streams that connect the inland region to the lake. We saw these features at Phnom Krom, Kompong Phluk and Kampong Khleang. We also saw a high radon peak at Prek Toal on the northwestern side of the lake towards Battambang (not shown). Since we usually operated out of Phnom Krom (near Siem Reap), we crossed this feature many times and observed that it appears to be permanent although the intensity (radon concentration and inventory) varies.

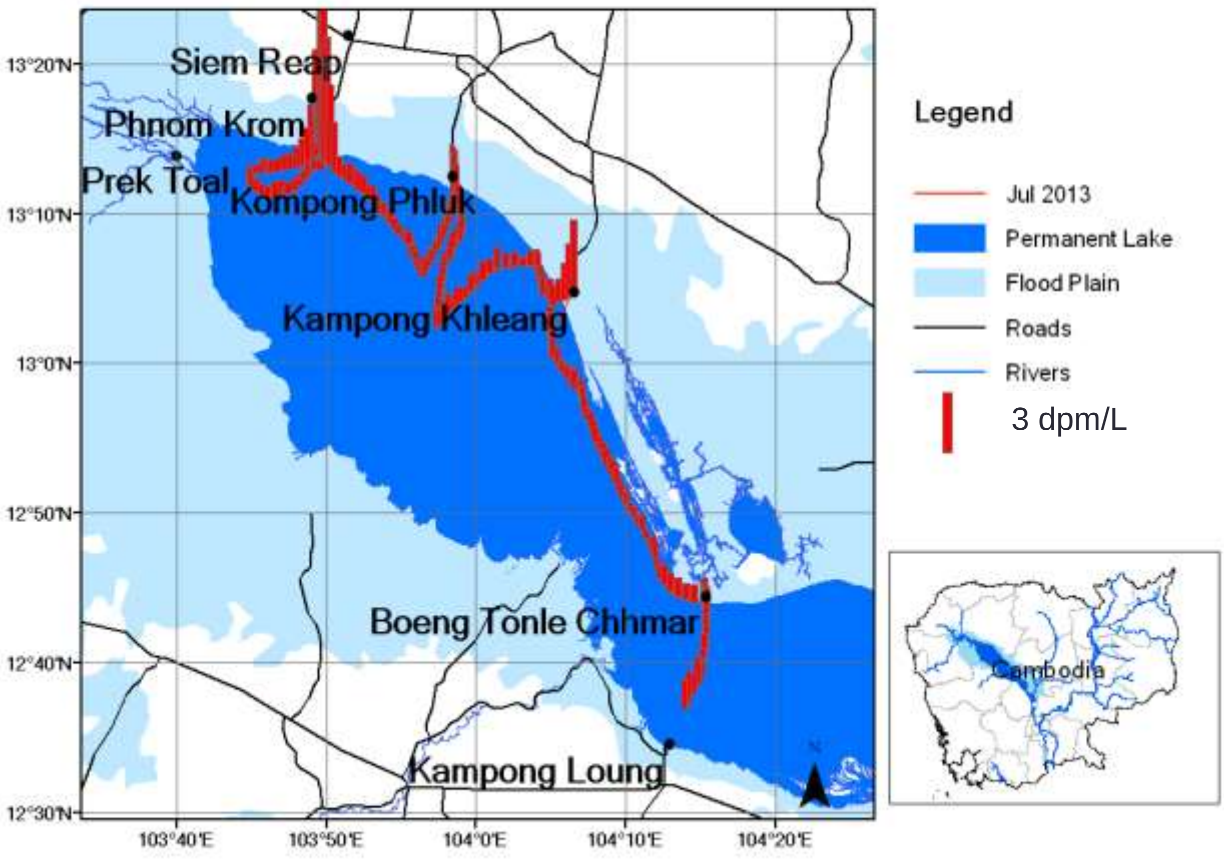

Fig. 5. Distribution of radon activities in the near surface waters of Tonle Sap Lake. Data collected during a fieldtrip from July 14-18, 2013.

When we look at the same radon data in an x-y plot versus cumulative distance surveyed over the 5-day long fieldtrip, we can see the sharp changes in the radon concentration as we crossed the various floodplain-permanent lake boundaries (**Fig. 6**). It is also clear from this plot that the conductivity changes most drastically at the same locations as the radon. When these features are looked at in more detail (**Fig. 7**), it is clear that the conductivity trends are exactly opposite than the radon features. The conductivity goes down sharply while the radon increases dramatically above the levels seen on either side of these features.

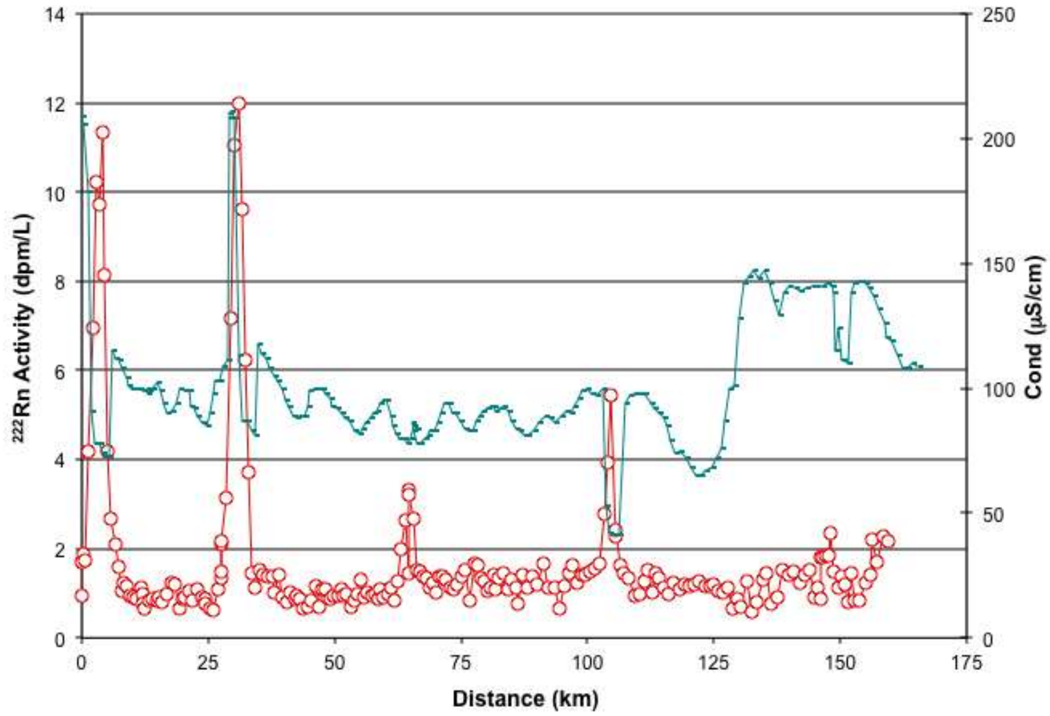

Fig. 6. Radon (open red circles) and conductivity (green line) versus cumulative distance during a survey July 14-18, 2013. The heavy dashed lines indicate the radon concentrations in different parts of the permanent lake. These radon concentrations were used in the mass balance model to estimate groundwater flows into TSL.

Groundwater entry into the lake at these points seems to be the only possible explanation for these features. A concentration of radium-rich minerals in the sediments could provide a source for the excess radon but would have no effect on the conductivity. In addition, we can see no reason why radium-rich minerals should concentrate preferentially along the boundary between the permanent lake and the floodplain. Instead, discharge of groundwater with relatively high radon and low conductivity seems like the most likely explanation. Indeed, analysis of approximately 40 wells in this area during an earlier study showed that the lowest conductivity groundwaters tended to have the highest radon concentrations.

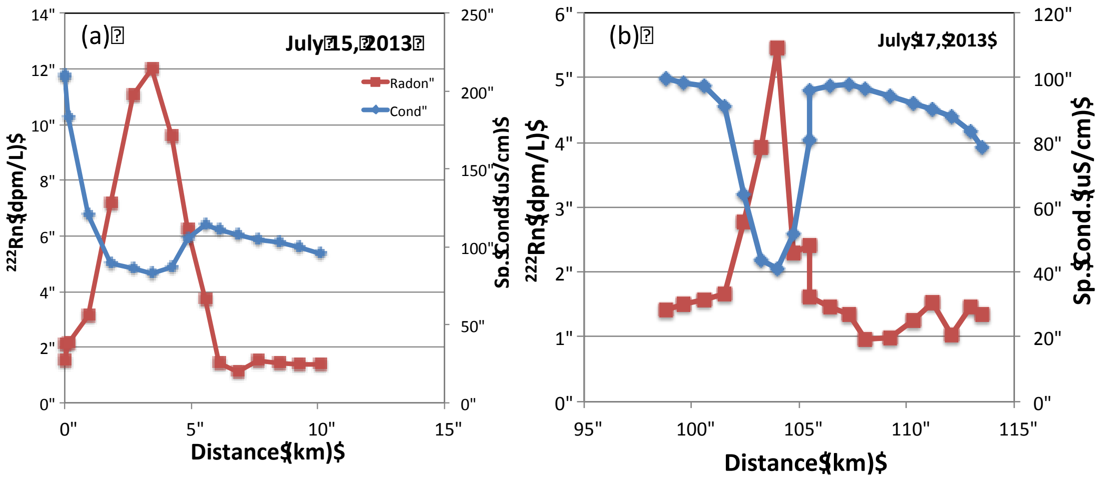

Fig. 7. Detailed views of radon and conductivity trends over hotspots observed at: (a) Phnom Krom; and (b) Kampong Khleang during July 2013.

Nutrient Trends

We analysed 190 water samples from 32 stations in the Mekong River and 104 stations in Tonle Sap Lake, during the project period. Averages of the river data show that some parameters are relatively constant, such as temperature and TDP, which dominates the TP in the three areas of the Mekong/Tonle Sap river system we measured (**Table 2**). Both the dissolved oxygen and pH of the Tonle Sap River are distinctly lower than the Mekong River stations. The suspended sediment concentration, on the other hand, is significantly lower in the TSR compared to the two Mekong River surveys.

Table 2. Statistics (average and standard deviation) for all field parameters, nutrients, and chlorophyll-a measured during three fieldtrips to the Mekong and Tonle Sap Rivers.

Measured Parameters	**Mekong River (Thailand) July 17-18, 2012**	**Mekong River (Laos) Oct. 24-24, 2012**	**Tonle Sap River Sept. 17-18, 2013**
Water Depth (m)	3.5±1.6	7.5±3.3	15.2±3.9
Conductivity (mS/cm)	172±48	308±3	147±2
Temperature (°C)	29.4±0.3	29.0±0.3	29.5±0.3
Dissolved Oxygen (mg/L)	7.4±1.2	6.8±0.1	4.9±0.6
pH	7.7±0.2	7.9±0.03	7.0±0.1
Suspended Sediment (mg/L)	154±33	94±11	28±46
DIP (µM)	0.45±0.26	0.82±0.10	0.64±0.08
TDP (µM)	0.88±0.23	0.94±0.14	0.74±0.08
DOP (µM)	0.43±0.08	0.13±0.12	0.09±0.08
TP (µM)	1.96±0.49	1.20±0.27	1.21±0.83
PP (µM)	1.08±0.47	0.26±0.20	0.47±0.82
NH_4 (µM)	n.d.	9.3±6.7	8.4±3.9
NO_3 (µM)	n.d.	30.9±3.4	14.1±2.0
DIN (µM)	n.d.	40.2±9.2	22.4±3.9
Chlorophyll-a (mg/L)	n.d.	n.d.	1.64±0.6

Notes: n.d. = not determined; $NO_3 = NO_2 + NO_3$

When the data for the lake surveys are examined in the same manner (**Table 3**), one sees that there are substantial ranges in some parameters depending upon the time of year when the sampling occurred. For example, suspended sediment (SS) concentrations are much higher in the June and July samplings when the water depth is lowest (average water depth only 0.9 m in June 2014). The conductivity shows a relatively narrow range between sampling periods as does the temperature and pH although the temperature range in the lake is much greater than observed in the river surveys. The DO is much lower in the November sampling when the depth was greater (average 6 m) and the temperature was highest. TDP dominates the TP in three out of the four sampling periods: January 2013, July 2013 and November 2014. The only exception was June 2014 when PP was the highest fraction of the total phosphorus.

Dissolved inorganic phosphorus (DIP) is the portion of total phosphorus that is most readily available for algal growth. Our measurements show that there is a wide range in the DIP fraction of the TP (**Fig. 8**). DIP varies from below detection in a few of the January 2013 samples to essentially 100% of the TP in a couple samples from the same period. The DIP in samples from the July 2013 sampling show a good correlation to TP while the June 2014 samples show a moderately good correspondence between the two fractions.

Table 3. Statistics (average and standard deviation) for all field parameters, nutrients, and chlorophyll-a measured during four fieldtrips to Tonle Sap Lake.

Measured Parameters	**Tonle Sap Lake**			
	Jan. 20-23 2013	**July 14-18 2013**	**June 24-26 2014**	**Nov. 7-10 2014**
Water Depth (m)	2.2±0.3	2.1±0.3	0.9±0.3	6.0±0.9
Conductivity (mS/cm)	178±27	135±27	137±31	178±19
Temperature (°C)	26.7±1.2	29.7±0.6	28.4±0.9	31.1±0.5
Dissolved Oxygen (mg/L)	6.8±1.9	6.8±0.7	6.0±1.0	4.3±2.2
pH	6.4±0.1	6.9±0.3	6.4±0.5	6.6±0.2
Suspended Sediment (mg/L)	56±83	809±530	1333±651	34±91
DIP (µM)	0.38±0.33	1.24±0.46	0.60±0.24	0.33±0.20
TDP (µM)	0.89±0.25	1.61±0.65	0.85±0.38	0.92±0.23
DOP (µM)	0.51±0.29	0.37±0.31	0.25±0.22	0.59±0.18
TP (µM)	1.18±0.20	2.08±0.49	3.06±0.73	1.47±0.43
PP (µM)	0.81±0.33	0.47±0.32	2.21±0.59	0.55±0.42
NH_4 (µM)	13.9±2.8	8.1±2.8	16.0±6.4	10.1±4.7
NO_3 (µM)	9.8±5.6	16.7±7.5	21.4±9.4	2.9±1.6
DIN (µM)	23.8±6.2	24.9±7.8	37.3±10.6	13.0±5.8
Chlorophyll-a (mg/L)	22.8±15.6	28.6±10.8	39.4±25.3	19.9±14.6

Notes: n.d. = not determined; $NO_3 = NO_2+NO_3$

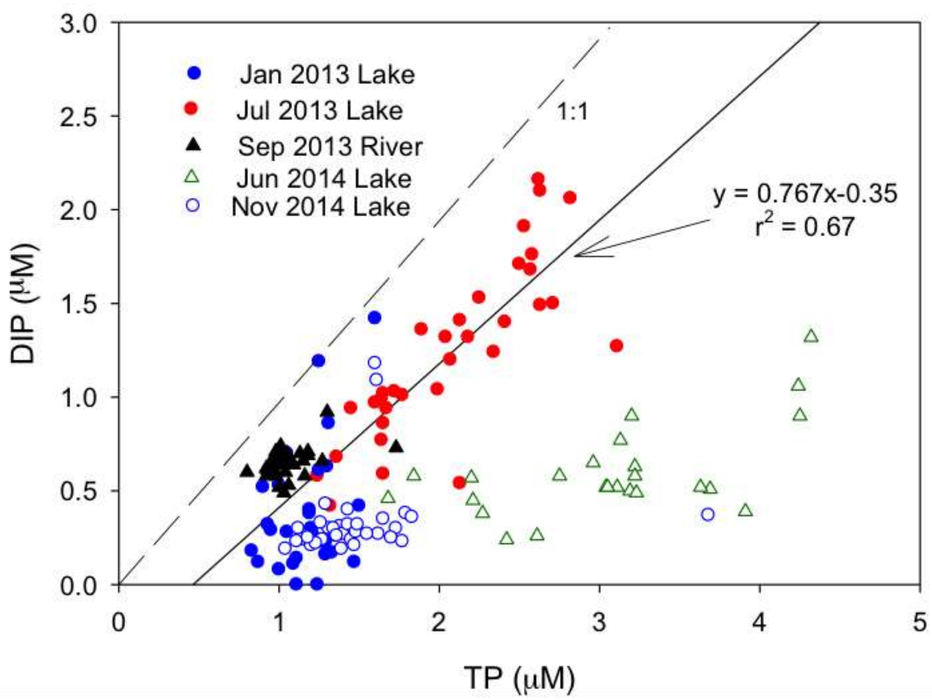

Fig. 8. DIP versus TP based on results from four samplings of Tonle Sap Lake and one sampling of Tonle Sap River. If all the TP consisted of DIP, the points would fall on the 1:1 line. The regression is shown for the July 2013 data set that covered more lake area than the other 3 surveys.

Station by station results of the relative P fractions show that the distribution of P species in the Mekong and Tonle Sap rivers is quite different than in TSL (**Fig. 9**). While DIP dominates the total phosphorus in almost every sample from the river sampling, the dominate P species in the lake varies between DIP and PP with the PP being highest at low water levels. DIP, PP and DOP make up about 33, 38 and 29% of the TP in the lake, respectively. This suggests that almost half of the DIP fraction in water entering from the Mekong has been taken up by phytoplankton and other primary producers in TSL. Hence, a rather high portion of PP is also revealed. PP is bound phosphorus that is only partly available to plant growth. The relatively high DOP fraction also indicates high organic content in the lake water. DOP is bioavailable for phytoplankton growth after bacterial decomposition. Biogeochemical processes in the system can affect concentrations of nutrients by transforming one chemical form to another as a result of environmental conditions or biological activity in the system. Sources of DIP to the system are both natural and human-derived, and include decaying organic material, fertilizers and other sources.

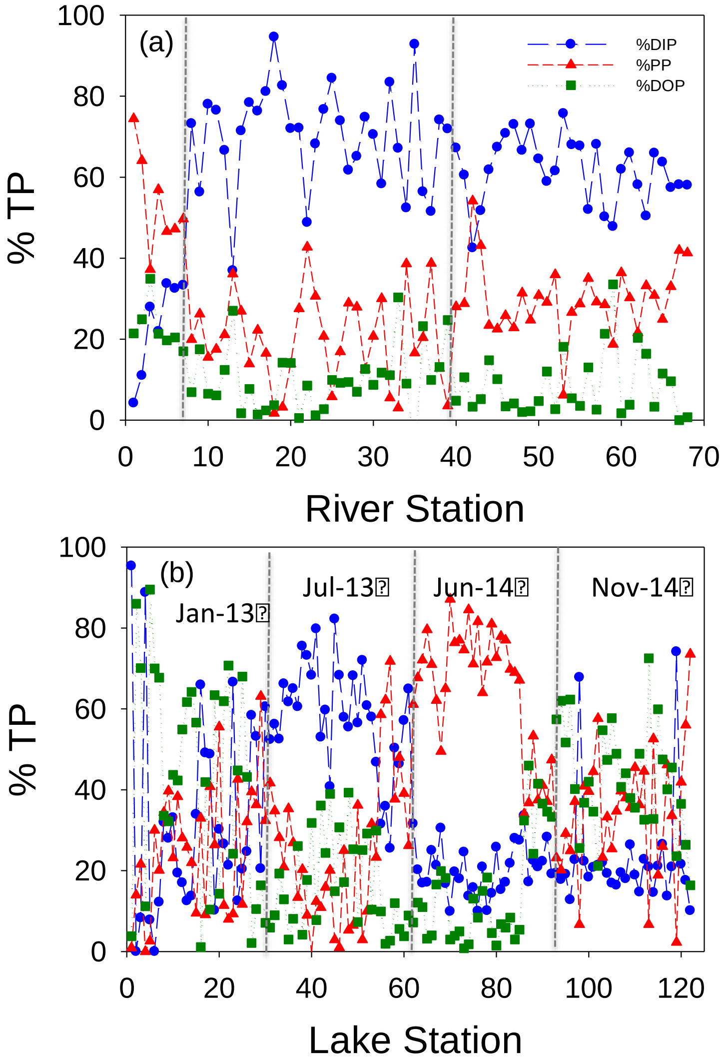

Fig. 9. Distribution of DIP (blue circles), DOP (green boxes) and PP (red triangles) as a percent of the total phosphorus (TP) in (a) the Mekong-Tonle Sap River system; and (b) Tonle Sap Lake. The vertical grey lines separate 3 field campaigns on the river system and 4 fieldtrips on the lake.

Another way to investigate the importance of particulate phosphorus is to plot PP versus TP for the various fieldtrips (**Fig. 10**). When this is done, it is obvious that the highest PP concentrations were observed in the June 2013 sampling when the water depth was less than 1 m on average. In addition, the PP forms a close relationship to the TP, representing a high fraction of the total. Although the concentrations are lower, it is interesting that the PP also forms a strong relationship to TP in the Tonle Sap River sampling (September 2013).

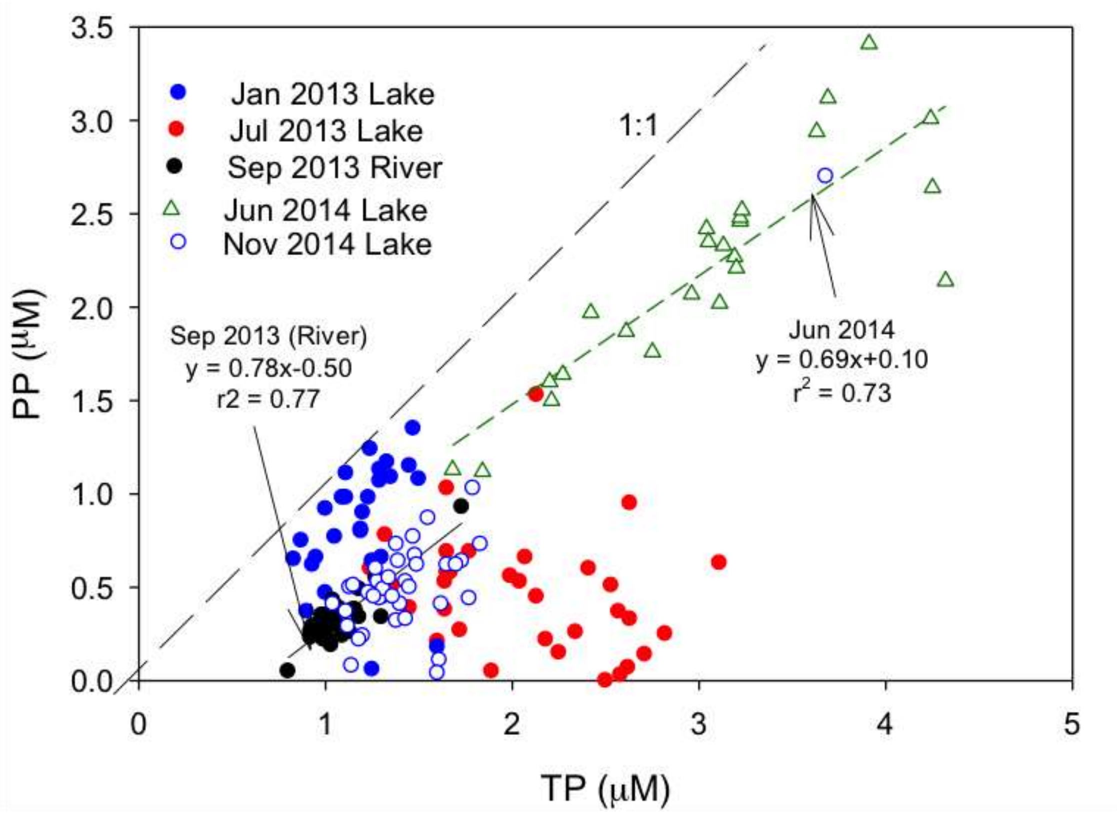

Fig. 10. PP versus TP based on results from four samplings of Tonle Sap Lake and one sampling of Tonle Sap River. If all the TP consisted of PP, the points would fall on the 1:1 line. The regressions are shown for the June 2014 (TSL) and September (TSR) data sets.

From the outset of this project, we have been assuming that the productivity of the lake was phosphorus limited, as are many fresh water systems. In order to evaluate that assumption, we examine the relationship between dissolved inorganic nitrogen (DIN) and DIP from all four of our lake samplings (**Fig. 11**). We note that with the exception of two samples from the January 2013 sampling that had DIP below detection, there is always some DIP present. We show a regression through the points from the July 2013 survey and observe that the intercept on the DIN axis is well above zero at 12.6 µM. This implies that even when the DIP reaches zero, there is still substantial DIN in the system, arguing against nitrogen limitation. We also show a reference line on the plot showing the N:P atomic ratio of 16:1, the so-called “Redfield Ratio” that represents the average N:P ratio in marine phytoplankton. While this is a freshwater system, the ratio is still useful as a framework for comparison. We note that with only a few exceptions, most of the data fall above the reference line indicating excess nitrogen. We also note that four out of the five samples from the July 2013 sampling and the single sample from the November 2014 survey that fall below the reference line have the highest DIP concentrations from those surveys. Interestingly, all of these samples with relatively high DIP concentrations and low N:P ratios are all from the same general area in the northeast part of the lake. This may be an area with higher than average groundwater discharge.

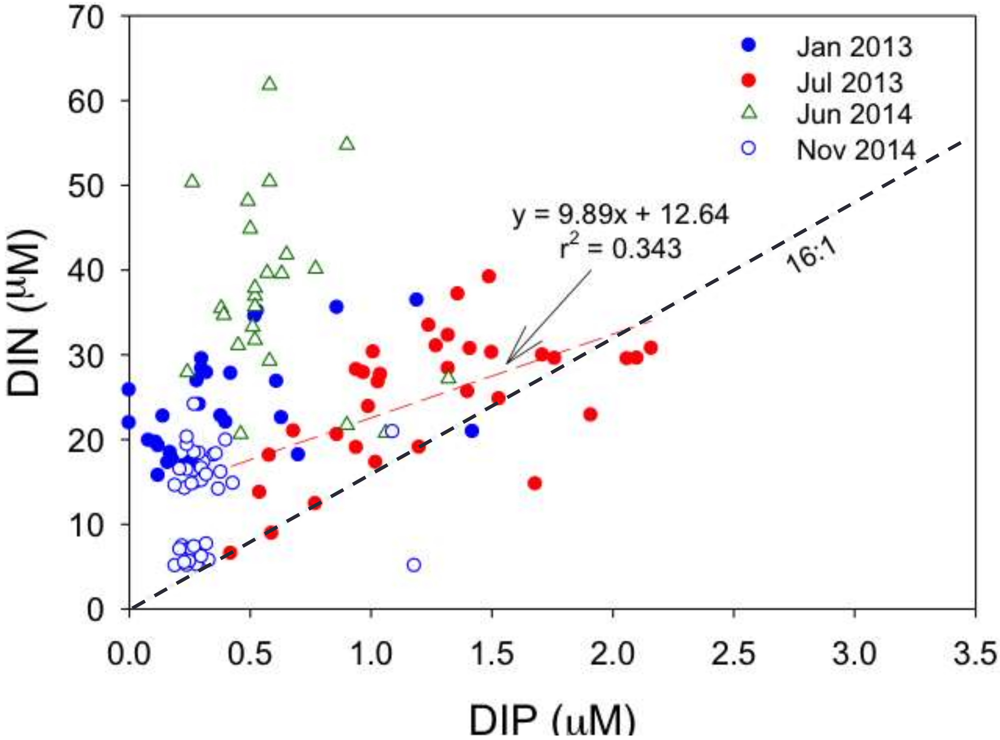

Fig. 11. DIN versus DIP in Tonle Sap Lake. The regression (dashed red line) is based on the July 2013 survey. The black dashed line represents the 16:1 N/P ratio for marine algae (Redfield Ratio).

Another way to examine nutrient limitation based on nutrient data is to look at the DIN:DIP ratios of all the lake samples. When we do this, the average DIN:DIP (N:P) ratio of all samples from TSL is 55±43. One criteria for a P-limited system is that the N:P ratio is greater than 22 (Healey, 1975). This thus supports the view that P is the limiting nutrient controlling the primary production of TLS Lake. In addition, a linear relationship between measured chl-a concentrations in TSL and DIP (**Fig. 12**), suggests that DIP controls the chlorophyll abundance in Tonle Sap Lake.

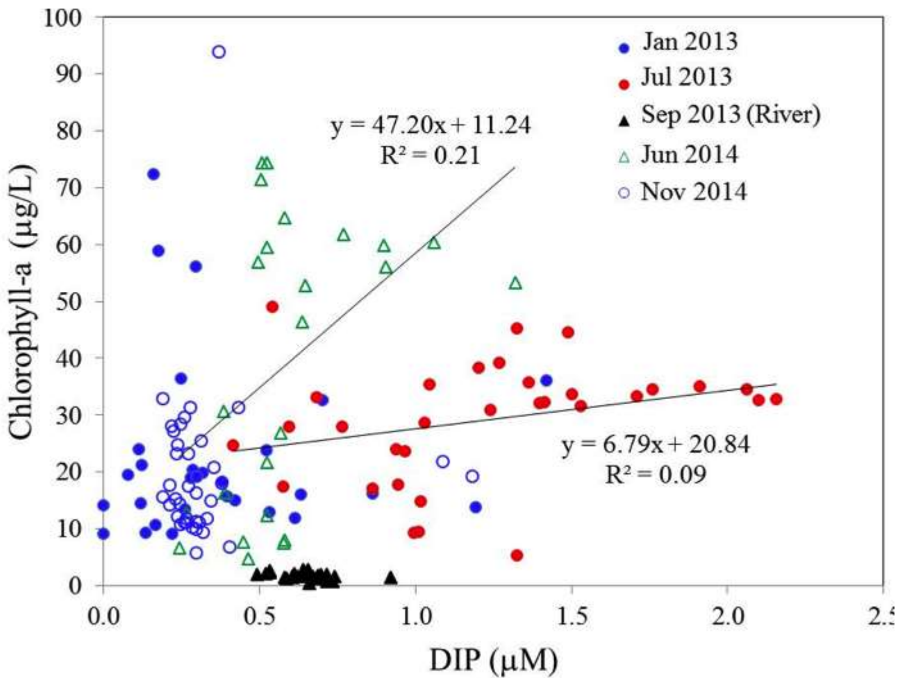

Figure 12. Relationship of chlorophyll-a to DIP in Tonle Sap Lake.

Chlorophyll-a (chl-a) is a proxy for algal biomass in a water body. Tonle Sap Lake can be considered a hyper-eutrophic water body because it maintains chl-a levels generally exceeding 25 µg/L. **Figure 13** provides a plot of chl-a distribution in TSL during the four surveys we carried out. The highest chl-a concentration was observed during the June 2014 survey when the water level was at its lowest (average water depth was 90 cm).

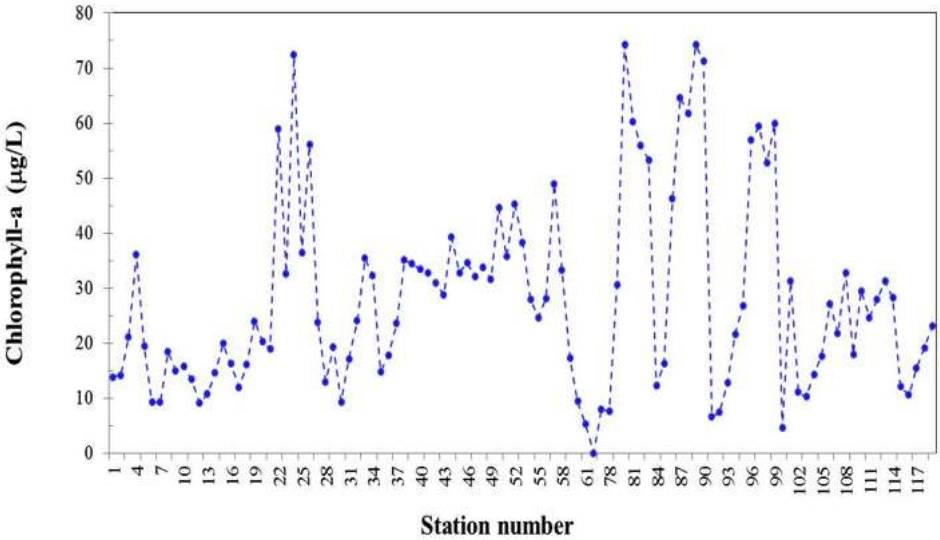

Fig. 13. Variation of chl-a in Tonle Sap Lake during our four lake surveys: January 2013 (station 1-29), July 2013 (station 30-61), June 2015 (station 77-100) and November 2014 (station 101-119).

Groundwater Inputs to Tonle Sap Lake

A listing of all the measured and derived parameters used for estimating the groundwater discharge via a mass balance model is given in **Table 4**.

Table 4. Measured and derived parameters used to estimate groundwater discharge into Tonle Sap Lake based on a radon mass balance. The 2009 and 2010 results are from a previous NGS study.

Measured Parameters	**Oct. 31 - Nov. 3 2009**	**Apr. 22 - 25 2010**	**Jan. 20 - 23 2013**	**July 14-18 2013**	**June 24-26 2014**	**Nov. 7-10 2014**
Water Temperature (°C)	29.6	31.9	27.4	30.6	29.2	31.4
Wind Speed (m/s)	3.2	2.5	3.6	3.9	2.5	1.3
Water Depth (m)	8.2	0.4	2.1	1.5	0.6	5.4
^{222}Rn Activity (dpm/L)	0.69	1.64	1.33	1.08	1.75	1.37
^{222}Rn Inventory (dpm/m^2)	5658	705	2727	1626	1073	7398
Lake Area (m^2)	1.33E+10	2.84E+09	6.75E+09	5.80E+09	3.31E+09	1.15E+10
Derived Parameters						
Atm. Evasion (dpm/m^2 day)	479	806	1085	1045	820	350
Diffusive Flux (dpm/m^2 day)	435	446	422	440	431	443
Decay (dpm/m^2 day)	1026	128	495	295	195	1342
Mixing (dpm/m^2 day)	31	4	15	9	6	41
River Flux (dpm/m^2 day)	-75	-29	-77	132	103	-113
Tributary Flux (dpm/m^2 day)	32	9	5	33	35	17
Total ^{222}Rn Flux to balance (dpm/m^2 day)	1144	512	1245	744	452	1386
Specific Advection (cm/day)	0.45	0.20	0.49	0.29	0.18	0.54
Total Discharge (m^3/s)	6.88E+02	6.58E+01	3.80E+02	1.95E+02	6.76E+01	7.21E+02
Total Discharge (m^3/day)	5.95E+07	5.69E+06	3.28E+07	1.69E+07	5.84E+06	6.23E+07
Total Discharge (km^3/y)	21.7	2.1	12.0	6.2	2.1	22.7

We used the radon inventories measured in the permanent lake during each of our surveys as the basis for the mass balance. While the data show that most of the radon from groundwater enters at the permanent lake/floodplain boundaries, the radon must be quickly transported to the open lake. Since we have good measurements over long survey distances in the permanent lake, we felt that variations in those radon inventories would represent a more dependable indicator of groundwater inputs than the few 'hotspots' we encountered at the floodplain boundaries.

The various fluxes were computed according to the equations shown in the section "Estimation of Groundwater Inputs" above. We have included 4 fieldtrips to TSL completed during the APN Project as well as two fieldtrips to TSL in 2009 and 2010 run during an earlier project sponsored by the National Geographic Society (NGS). The range of most fluxes on a per unit area basis is quite high with the exception of the radon inputs via diffusion, which would be expected to be reasonably constant in a tropical environment without wide differences in temperature throughout the year (**Fig. 14**). The range of radon inventories varied over about an order of magnitude while the radon concentrations changed less than a factor of three. This is an effect of the extreme changes in water level over the hydrologic cycle.

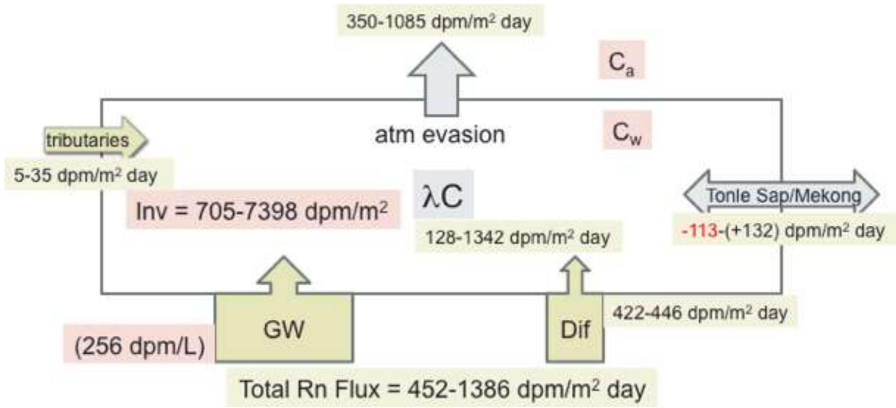

Fig. 14. Radon mass balance ranges measured during 6 fieldtrips (2 from NGS study; 4 from APN project) to Tonle Sap Lake. C_a and C_w represent radon concentrations in the atmosphere and water column, respectively. Inv represents radon inventories (radon concentration x water depth). GW and Dif stand for input fluxes of radon via groundwater and diffusion from sediments.

When we plot the estimated discharges by month over the hydrologic year (lowest water level to highest and back to lowest; May to April) we see that the maximum discharge occurs in November after the lake has started to drain (**Fig. 15a**). The lowest discharges are at the lowest water levels in June and April. In order to estimate the approximate discharges in the months without any measurements, we fit the 6 months with groundwater estimates to a 3-parameter Gaussian peak fitting equation. This resulted in a good fit to the observed data (r^2 = 0.996). Using this fit, we added in estimates of the missing months so we now have monthly estimates of groundwater discharge based on average water levels and lake areas (**Fig. 15b**).

If we plot these results over a full hydrologic year together with average TSR and tributary discharge values, an interesting pattern emerges (**Fig. 16**). The discharge from TSR peaks in August, the tributaries show the maximum flow in October, and the groundwater discharge peaks still later in November. Note that while the flow rates are lower than TSR in the tributaries, the flow is always positive, i.e., flow into the lake. TSR flow, on the other hand, flows out of the lake from about October to April. The lag in the inflow from the tributaries is likely due to different monsoonal weather patterns in the local region compared to further up the Mekong River Basin where the wet monsoon begins somewhat earlier. The still later peak flow in the groundwater is likely a result of the increase in hydraulic head as the lake begins to drain in late October. Much of the groundwater that is discharged into the lake is probably re-circulated lake water that entered the subsurface when the lake level was high. This is known as "bank storage" in hydrology. When the lake starts to drain, the surface water flows faster than the groundwater setting up a positive hydraulic gradient between the groundwater level and the now lower lake level. This will continue as long as the lake continues draining.

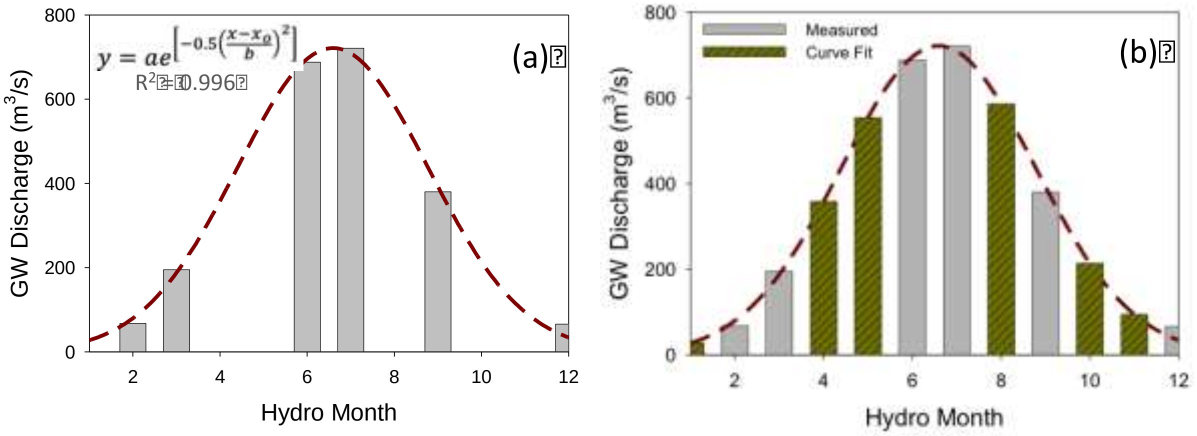

Fig. 15. (a) Groundwater estimates over a hydrological year based on data collected during six fieldtrips to Tonle Sap Lake. The dashed line is a best fit to the estimates shown. (b) Groundwater estimates for a full hydrological year based on interpolations provided by a 3-parameter Gaussian peak equation.

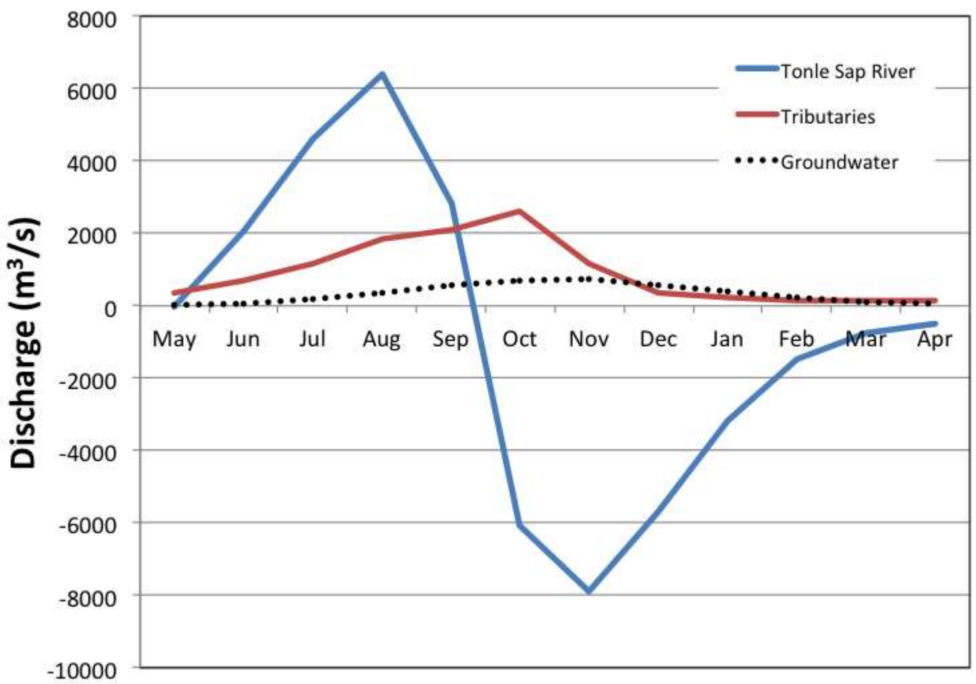

Fig. 16. Discharge trends into and out of Tonle Sap Lake from the Tonle Sap River, tributaries, and groundwater. Positive values represent flow into TSL while negative values are for flows exiting the lake through the TSR. Data for TSR and tributaries compiled by M. Kummu (pers. comm.). Groundwater results from this study.

Sources of Water and DIP to Tonle Sap Lake

Water Budget: Based on data from Kummu et al. (2013) and our data presented here, we have constructed a water budget for TSL (**Fig. 17**). The budget is based on average river, tributary and groundwater monthly flows (**Fig. 16**) as described earlier. Notice that while the TSR is the main water source during the wet season (42.2 km^3/yr) that even more water leaves the lake via this river during the dry season (67.3 km^3/yr). Thus, the TSR actually represents a net loss of water from the lake over an entire hydrological year. This loss is estimated at 25.1 km^3/yr that is balanced mainly by flow from the tributaries (29.1 km^3/yr). By integrating our estimated monthly groundwater flows over the entire year, we calculate that the average groundwater flow into TSL is about 10.4 km^3/yr. This flow is substantial, amounting to about 25% of the water from the TSR during the wet season and about 35% of the tributary flow over the entire year.

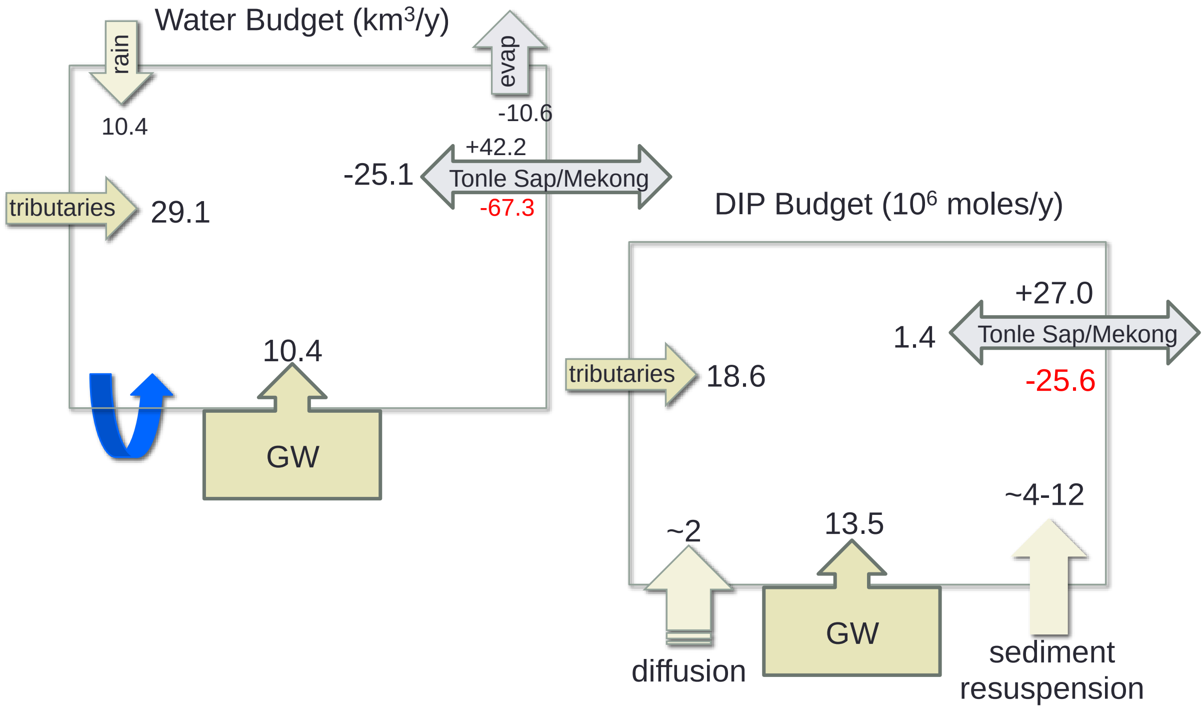

Fig. 17. Estimated water and DIP budgets for Tonle Sap Lake.

If one does not consider groundwater flow, the water budget does not quite balance. Evaporation closely matches direct rainfall to the lake but there is an apparent additional 4 km^3/y flowing into the lake than leaving via the TSR (29.1 – 25.1 = 4 km^3/yr). At maximum flood stage, usually sometime in October, the volume of TSL is about 60 km^3 so the 4 km^3 discrepancy is only about 7% of the total. The imbalance is much larger, of course, at the lowest stage of the lake when the volume is only about 2 km^3. Water budgets such as the one described here often display this type of imbalance. All the terms in the budget have their own uncertainty and these uncertainties are propagated when values are combined. Another relevant point is that the budget presented is for 'average' conditions. While conditions in the Mekong-Tonle Sap system are relatively consistent over time, no year will be exactly 'average.'

It appears that when one adds in the groundwater estimate (10.4 km^3/yr), the imbalance gets worse, rather than better. We propose that the reason for this is that much of the groundwater flow is actually re-circulated lake water, i.e., water that infiltrated the shallow subsurface when the lake level is high and later discharges to the lake when the level is dropping. So this process would not contribute anything to the water balance. Unfortunately, we do not have the data necessary to work out how much of the groundwater discharge is re-circulated lake water versus upland groundwater entering the lake for the first time. Either way, the groundwater contribution may be an important source of nutrients to the lake.

Sediment Resuspension: During the low level period, the lake is very shallow and sediment resuspension by wind and other forms of turbulence is very common. We have shown earlier that DIP concentrations correlate to suspended sediment concentrations in June and July while samplings in January and November, when the lake is significantly deeper, showed no such relationships. We thus assume that there is release of DIP from suspended sediment and that this process occurs mainly during the low water period (May-August).

In order to estimate this release, we rely on data from the sediment release experiments. Taking the results from the DIP concentration versus time plots (not shown), we can relate the flux of DIP release and equilibrium value of DIP to the suspended sediment concentrations (**Fig. 18**). We then compare the observed concentrations of DIP from each of our lake samplings to the calculated equilibrium values based on the observed SS concentrations. We find that the observed DIP values are lower than the estimated equilibrium values only during the low water periods we sampled (June and July). We further assume that the difference in DIP between the observed and equilibrium values will be released to the lake water. Multiplying this concentration difference (μM/L) by the estimated lake volume (L) provides an estimate of the total release of DIP for that time interval. We estimated a total release of DIP by resuspension of sediments in June of 6.42 x 10^6 moles and 1.46 x 10^6 moles for July. Extrapolating to the other 2 months with low water and likely resuspension results in a range of DIP release to the entire lake from 10.8 x 10^6 to 20.7 x 10^6 moles/year.

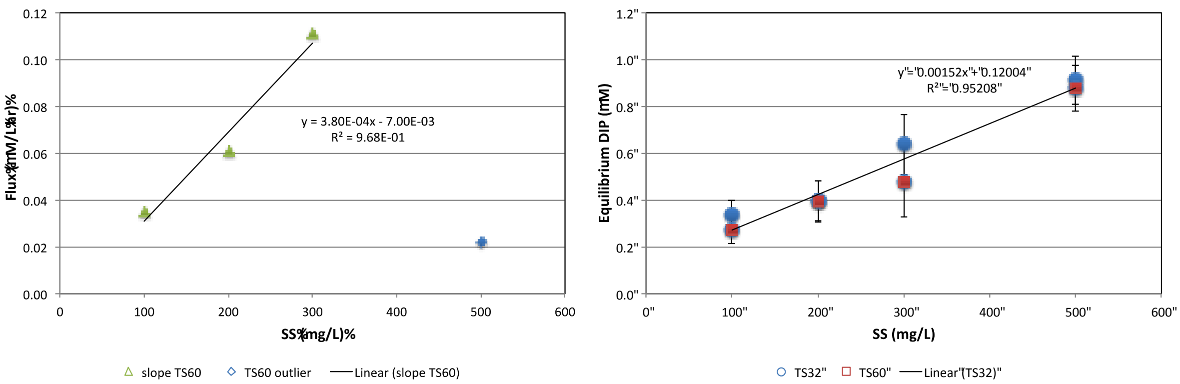

Fig. 18. Release rate of DIP as a function of SS concentration (left panel) and equilibrium DIP concentration as a function of SS concentration. These results are from the sediment release experiments.

Diffusion of DIP from Sediments: In order to estimate the DIP input via diffusion, we again rely on the P release experimental results. By extrapolating the relationship between DIP equilibrium values and SS concentrations to the point that simulates Tonle Sap wet sediment with about 40% moisture, we calculate an equilibrium pore water DIP value of about 3.4 μM. Using a diffusion coefficient for DIP from the literature (Boudreau, 1996) of 7.69 x 10^{-6} cm^2/s, and a sediment depth to equilibrium of 10 cm, we obtain a diffusive rate of about 2 $μM/m^2$ day or about 2 x 10^6 moles/year for the entire permanent lake.

DIP Inputs to Tonle Sap Lake: Using the average water flow information presented above and our data for the average DIP concentrations in the TSR and lake, we have constructed an estimated DIP budget for TSL (**Fig. 17**). While the TSR has a negative water contribution to the lake, the net DIP input is positive at 1.4 x 10^6 moles/yr. This results from the higher DIP concentrations in the TSR (average measured during our September 2013 fieldtrip = 0.64 ± 0.08 µM; n = 30) than in TSL. Tributaries, assumed to have the same average DIP concentration as the TSR, contribute the largest amount at 18.6 x 10^6 moles/yr. The groundwater contribution is substantial, amounting to 13.5 x 10^6 moles/yr, more than 30% of the total calculated DIP flux into the lake. Our estimated input of DIP by diffusion appears to be of only minor importance but the flux from resuspension may be substantial and clearly of more importance during low water periods. Any flux from the sediment, whether from resuspension or diffusion, would consist of re-generated phosphorus. However, river and tributary fluxes would represent new P and groundwater inputs would be a combination of both new and re-cycled P.

Results of System Dynamic Modelling

Kummu and Sarkkula (2008) compiled a cumulative impact assessment of the construction for large-scale hydropower dams and reservoirs in the upper part of the Lower Mekong Basin. They based their assessment of the impact on the flow to TS Lake by reviewing reports of the Mekong River Commission (MRC) and the Asian Development Bank (ADB). The authors predicted that over a 20-year time frame with a high development scenario, the maximum water level of the lake will be lowered by 0.36 to 0.54m and the minimum water level of the lake would increase by as much as 0.6 m. The authors thus predicted that there would be a change in water discharge to the lake. Lauri et al. (2012) also wrote that the simulated change in discharge at Kratie (Cambodia) between the baseline (1982–1992) and projected time period (2032–2042) ranges from −11% to +15% for the wet season and −10% to +13% for the dry season. Our approach was to build a systems dynamic model that can be tested against time series data available at different times (2001 and 2013). The hope was that the SD model would be capable of reproducing the dynamic behaviour of particulate and dissolved phosphorus.

The main variables of the model are particulate and total dissolved phosphorus (TDP) in the lake water column. While the model generated the behaviour of TDP of the lake reasonably well, the model failed to explain the peak of the particulate phosphorus in the lake in May despite many simulations with different values of parameters of the model. **Figures 19 and 20** show predictions of the model together with actual PP and TDP measurements in 2001 for comparison while **Figures 21 and 22** show the predictions of the model with actual PP and TDP measurements in 2013. The model agreed reasonably well with the trends for TDP and PP in the water column in 2001 and particularly well for the behaviour of PP in 2013. Unfortunately, the model did not work well to predict the TDP in the water column during 2013.

Limitations of the model and associated results can be linked to the modelling process and the data used to calibrate and provide predictions of nutrient conditions. For example, the completely mixed water column assumption used in the model may be violated in Tonle Sap Lake during the wet season when the lake is deep enough for thermal stratification. This could isolate much of the lake bottom from interactions with the surface layer. Also, there are limitations with the data used in the modelling process. This study assumed nutrient concentrations from the main river channel and tributaries to the TS Lake are the same while this is not known. However, the results are encouraging enough to merit further investigation. A full description of the SD modelling attempts, including relevant stock and flow diagrams and governing equations, is contained in the appendix of this report.

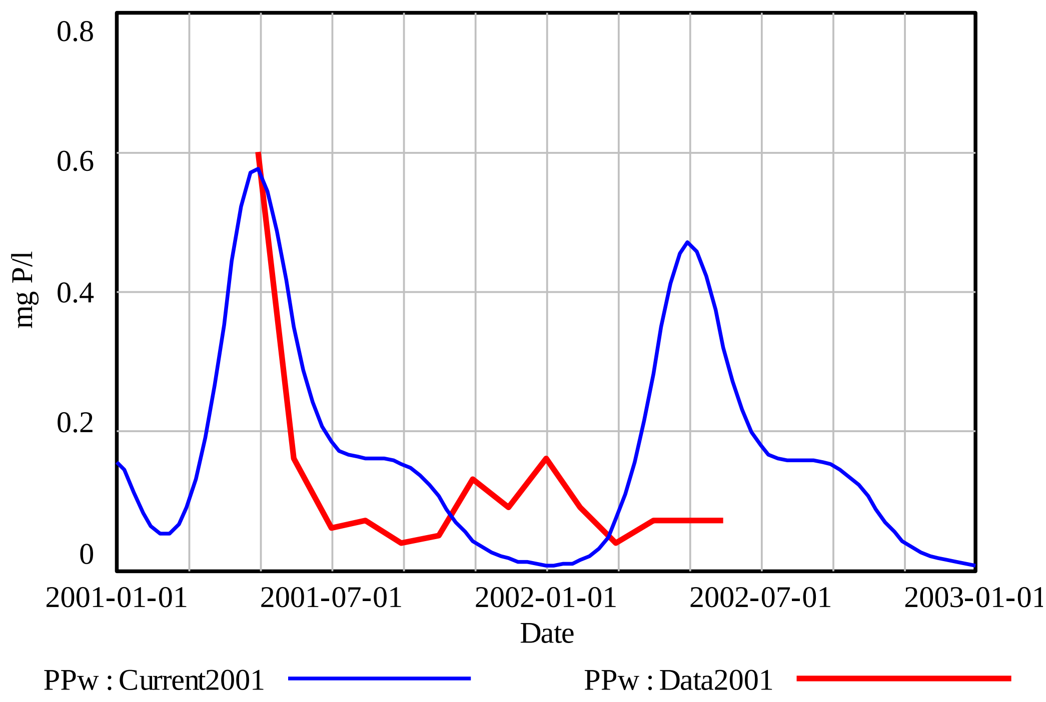

Fig. 19. Simulated behaviour of particulate phosphorus (PPw) in 2001.

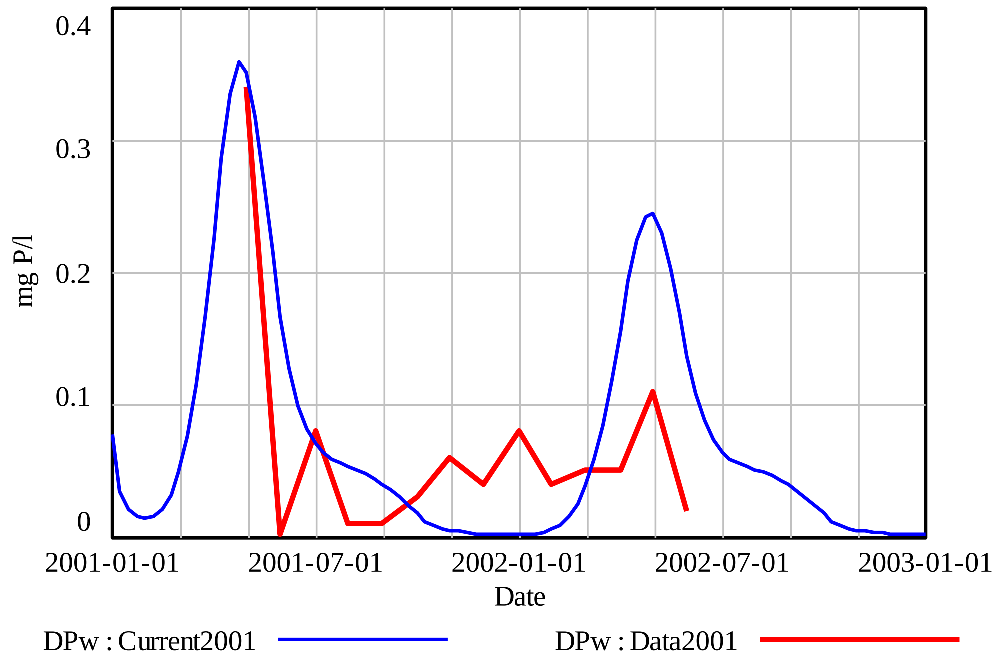

Fig. 20. Simulated behaviour of dissolved inorganic phosphorus (DIPw) in 2001.

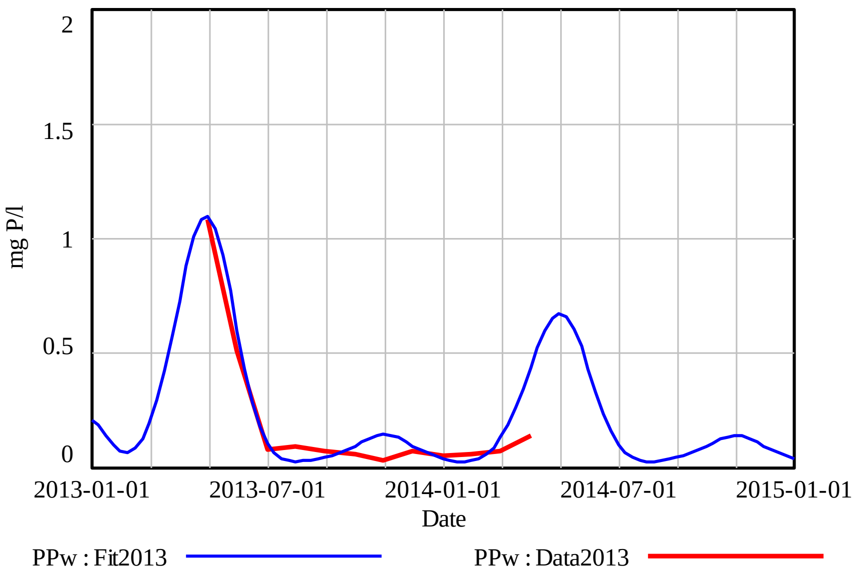

Fig. 21. Simulated behaviour of particulate phosphorus (PPw) in 2013.

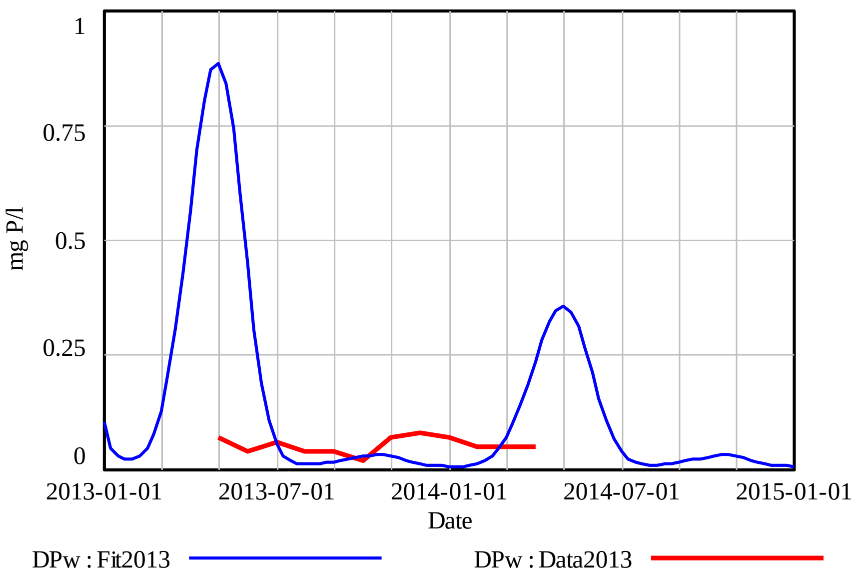

Fig. 21. Simulated behaviour of dissolved inorganic phosphorus (DIPw) in 2013.

5. Conclusions

A radon mass balance model indicates that the groundwater flow to Tonle Sap Lake is about 10.3 km^3/yr. While much of this groundwater is likely re-circulated lake water ('bank storage'), it may still be important as a nutrient contributor. As lake water penetrates the subsurface, nutrients will be released from the solid phases of the shallow aquifer by organic matter decomposition and other processes. In addition, some upland groundwater will contribute to this total and add some amount of new nutrients to the lake. Our results suggest that the DIP contribution to TSL is more than 30% of the average inflows from the TSR, tributaries and groundwater combined. Inputs from sediments, another potentially large source, have also been estimated. Diffusion is likely of minor important but inputs of DIP from resuspension of bottom sediments may be substantial. We have not attempted to quantify inputs of P from sewage, fertilizers, and other human sources in this study.

Our nutrient results are consistent with the concept that Tonle Sap Lake is phosphorus limited. The average N:P ratio from all of our samplings was 55±43, well over the 22:1 ratio often cited as a criteria for phosphorus limitation. In addition, a plot of DIN versus DIP of lake water shows that most samples contain 'excess' nitrogen relative to average algal requirements.

6. Future Directions

The groundwater end-member value (256 dpm/L) is based on several sediment equilibration results run in the laboratory and reported in Chanyotha et al. (2014). If one assumed that 100% of the groundwater was derived from upland sources and none of the discharging groundwater was recycled lake water, a more appropriate end-member value would be 660 dpm/L, the average groundwater value obtained by analysing dozens of shallow wells (Burnett et al., 2013). If that were the case, the groundwater inflow would be about a factor of two smaller, although still significant.

In order to obtain a more accurate end-member radon concentration, we would need to obtain information on the relative proportions of re-circulated versus pure upland groundwater. This is not a simple task but could be done by sampling shallow groundwater on the floodplain during the period when the lake is draining. The samples could then be analysed for parameters that could be used as source indicators such as stable isotopes or radium isotope ratios in addition to radon.

We have limited this study to an investigation of natural sources of phosphorus to Tonle Sap Lake. However, with increased development in the basin, anthropogenic sources will likely become increasingly more important. Thus, human activities such as sewage inputs to the lake and use of fertilizers should be monitored as these will likely increase in the years ahead.

We would also like to point out that there is a need to improve upon the water quality monitoring being conducted in the Mekong River and Tonle Sap systems. While the MRC does conduct routine water quality monitoring, some of the results we have examined display discrepancies that are difficult to understand. For example, in some periods both TP and DIP (called 'PO_4' by the MRC) have been analysed while in other periods only TP is being reported. In other cases, examination of time series data has shown unusual shifts in the data that do not look natural. We suspect that these represent changes in laboratory procedures, personnel, or contract laboratories rather than actual shifts in the nutrient environment.

Acknowledgements

We have many people to thank for their cooperation and assistance during this project. Bunseang Suy (Tonle Sap Rural Water Supply, Battambang, Cambodia) was extremely helpful in the field and for arranging many of the logistics for our fieldtrips. Dr. Matti Kummu (Water and Development Research Group, Aalto University, Finland) was kind enough to provide us with his data on lake water levels, river discharge values, etc., which greatly assisted our modelling efforts. Ms. Sophea Nhim (Ministry of Water Resource and Meteorology, Phnom Penh) supervised the sampling and analysis of the samples from the one-year time series. Dr. Jariya Boonjawat (START and Chulalongkorn University) allowed us to post project plans on the START website. Finally, we thank the following for their very capable assistance in the field: Dr. Supitcha Chanyotha, Ratsirin "Prae" Supcharoen, Rawiwan "O" Kritsananuwat, Pongjit "Tarn" Jaiboon (all from Chulalongkorn University), Butsawan "Nok" Bidorn (Florida State University), and Dalasack Xayyasouk (National University of Laos).

References

Baines, S.B. and M.L. Pace, 1994. Relationships between suspended and particulate matter and sinking flux along a trophic gradient and implications for the fate of planktonic primary production. Can. Jour. Fish. Aquatic Sci. 51: 25-36.

Baldwin, D.S., A.M. Mitchell, and G.N. Rees, 2000. The effect of in situ drying on sediment phosphate interactions in sediments from an old wetland. Hydrobiologia. 431, 3-12.

Boudreau, Bernard P., 1997. Diagenetic Models and their Implementation. Springer-Verlag, Berlin. 414 pp. ISBN 3-540-61125-8.

Briggs, S.V., M.T. Maher, and S.M. Carpenter, 1985. Limnological studies of waterfowl habitat in south-western New South Wales. I. Water Chemistry. Australian Journal of Marine and Freshwater Research. 36, 59-67.

Burnett, W.C., G. Kim, and D. Lane-Smith, 2001. A continuous radon monitor for assessment of radon in coastal ocean waters. Journal of Radioanalytical and Nuclear Chemistry, 249, 167-172.

Burnett, W.C., R.N. Peterson, S. Chanyotha, G. Wattayakorn, B. Ryan, 2013. Using high-resolution in-situ radon measurements to determine groundwater discharge at a remote location: Tonle Sap Lake, Cambodia. Journal of Radioanalytical and Nuclear Chemistry, 296, 97-103.

Chanyotha, S., C. Kranrod, and W.C. Burnett, 2014. Assessing diffusive fluxes and pore water radon activities via a single automated experiment. Journal of Radioanalytical and Nuclear Chemistry, 301, 581-588.

Charette, M.A., W.S. Moore, and W.C. Burnett, 2008. Uranium- and thorium-series nuclides as tracers of submarine groundwater discharge. Chapter 5 In: "U-Th Series Nuclides in Aquatic Systems," (eds. S. Krishnaswami and J. Kirk Cochran), Elsevier, Amsterdam, 155-191.

Clesceri, L.S., A.E. Greenberg, and A.D. Eaton, (eds.), 1998. Standard Methods for the Examination of Water and Wastewater, 20th ed., Washington, D.C., American Public Health Association.

Corbett, D.R., W.C. Burnett, P.H. Cable, and S.B. Clark, 1998. A multiple approach to the determination of radon fluxes from sediments. Jour. Radioanalytical & Nuclear Chemistry, 236, 247-252.

Day, B.D., D.A. Hodell, M. Brenner, et al., 2011. Middle to late Holocene initiation of the annual flood pulse in Tonle Sap Lake, Cambodia. Journal of Paleolimnology, 45, 85-99.

Dulaiova, H., R. Peterson, W.C. Burnett, and D. Lane-Smith, 2005. A multi-detector continuous monitor for assessment of ^{222}Rn in the coastal ocean. Journal of Radioanalytical and Nuclear Chemistry, 263(2), 361-365.

Elser, J.J. et al., 2007. Global analysis of nitrogen and phosphorus limitation of primary producers in freshwater, marine and terrestrial ecosystems. Ecol. Lett. 10, 1135-1142.

Fabre, A.,1988. Experimental studies on some factors influencing phosphorus solubilization in connexion with the drawdown of a reservoir. Hydrobiologia, 159, 153-8.

Ford, A., 1999. Modeling the environment: An introduction to system dynamics models of environmental systems. Island Press.

Healey, F P., 1975. Physiological indicators of nutrient deficiency in algae. Fish. Mar. Serv. Res. Div. Tech. Rep. 585: 30.

Hecky R.E. and P. Kilham 1988. Nutrient limitation of phytoplankton in freshwater and marine environments: a review of recent evidence on the effects of enrichment. Limnol. Oceanogr. 33, 796–822.

Junk, W.J., P.B Bayley, and R.E. Sparks, 1989. The flood pulse concept in river-floodplain systems. Canadian Special Publication in Fisheries and Aquatic Science 106, 110–127.

Junk, W.J., 1999. The flood pulse concept of large rivers: learning from the tropics. Arch. Hydrobiol. Suppl. 115/3, 261-280.

Kummu, M., and J. Sarkkula, 2008. Impact of the Mekong River flow alteration on the Tonle Sap flood pulse. Ambio*,* 37(3): 185-192.

Kummu et al., 2013. Water balance analysis for the Tonle Sap Lake–floodplain system. Hydrological Processes, DOI: 10.1002/hyp.9718.

Lamberts, D., 2006. The Tonle Sap Lake as a productive ecosystem. Water Resources Developments, 22, 481-495.

Lamberts, D., et al., 2007. Mekong River Basin development and Tonle Sap Lake productivity: current knowledge and future challenges. 2nd International Symposium on Sustainable Development in the Mekong River Basin, 187-195.

Lauri H., H. de Moel, P.J. Ward, T.A. Rasanen, M. Keskinen, and M. Kummu, 2012. Future changes in Mekong River hydrology: impact of climate change and reservoir operation on discharge. Hydrology and Earth System Sciences, 16: 4603–4619.

Macintyre, S., R. Wanninkhof, and J.P. Chanton, 1995. Trace gas exchange across the air-sea interface in freshwater and coastal marine environments. In: P.A. Matson, R.C. Harriss (eds.) Biogenic Trace Gases: Measuring Emissions from Soil and Water, Blackwell Science Ltd. 52-97.

Mitchell, A., and D.S. Baldwin, 1998. Effects of desiccation/oxidation on the potential for bacterially mediated P release from sediments. Limnology and Oceanography, 43, 481–487.

Mitchell, A.M., and D.S. Baldwin, 1999. The effects of sediment desiccation on the potential for nitrification, denitrification, and methanogenesis in an Australian reservoir. Hydrobiologia, 392: 3–11.

MRC (Melong River Commission), 2005. Overview of the Hydrology of the Mekong Basin. Mekong River Commission, Vientiane (Laos), November 2005, 73 p.

Ohtaka, A., R. Watanabe, S. Im, R. Chhay and S. Tsukawaki, 2010. Spatial and seasonal changes of net plankton and zoobenthos in lake Tonle Sap, Cambodia. Limnology 11, 85-94.

Qiu, S. and A. J. McComb, 1994. Effects of oxygen concentration on phosphorus release from reflooded air-dried wetland sediments. Australian Journal of Marine and Freshwater Research, 45, 1319–1328.

Qiu, S. and A.J. McComb, 1996. Drying-induced stimulation of ammonium release and nitrification in re-flooded Lake sediment. Marine and Freshwater Research, 47, 531–536.

Sarkkula, J., J. Koponen, M. Kummu, et al., 2003. Modelling Tonle Sap for Environmental Impact Assessment and Management Support. Final Report to the Mekong River Commission, 110 p.

Sartory, D.P. and J.U. Grobbelaar, 1984. Extraction of chlorophyll-a from freshwater phytoplankton for spectrophotometric analysis. Hydrobiologia, 114, 177-187.

Schindler, D.W., 1970. Evolution of phosphorus limitation in lakes. Science 195, 260–262.

Schindler D.W., 1978. Factors regulating phytoplankton production and standing crop in the world's freshwaters. Limnol . Oceanogr. 23, 478-486.

Søballe, D.M. and B.L. Kimmel, 1987. A large-scale comparison of factors influencing phytoplankton abundance in rivers, lakes, and impoundments. Ecol. 68: 1943-1954.

Sterner, R.W., 2008. Review Paper: On the phosphorus limitation paradigm for lakes. Internat. Rev. Hydrobiol. 93 (4-5), 433-445.

Strickland, J.D.H., Parsons, T.R., 1972. A Practical Handbook of Seawater Analysis. Fisheries Research Board of Canada Bulletin: 157, Ottawa.

Turner, B.L. and P.M. Haygarth, 2001. Phosphorus solubilization in rewetted soils. Nature, 411, 258.

Weigel, F., 1978. Radon. Chemiker-Zeitung, 102 (9), 287−299.

Appendices

Appendix 1. Field and laboratory parameters for Mekong River sampling in Thailand during July 17-18, 2012.

Sample	Date	Latitude	Longitude	River	Sampling	Specific	DO	Temp	pH	SS	DIP	TDP	DOP	TP	PP
		ºN	ºE	depth (m)	depth (m)	conductivity	mg/L	ºC		mg/L	(µM)	(µM)	(µM)	(µM)	(µM)
												filtered		unfiltered	
MR1S	17-Jul-12	16.601	104.736		1.0	126		29.1	7.65	147	0.11	0.69	0.57	2.69	2.00
MR1B	17-Jul-12				4.0	126	6.14	29.4	7.68	210	0.20	0.66	0.45	1.83	1.17
MR2S	18-Jul-12	17.487	104.789	5.2	1.0	145	6.33	29.3	7.53	139	0.37	0.84	0.47	1.34	0.50
MR2B	18-Jul-12				5.0	146	6.67	29.3	7.47	179	0.35	0.69	0.34	1.59	0.91
MR3S	18-Jul-12	18.385	103.633	3.5	1.0	208	8.83	29.9	7.80	119	0.61	0.97	0.36	1.81	0.84
MR3B	18-Jul-12				3.0	208	8.39	29.8	7.83	122	0.62	1.02	0.39	1.92	0.91
MR4S	18-Jul-12	17.885	102.745	1.9	1.0	248	8.17	29.3	8.06	161	0.85	1.28	0.43	2.55	1.27
					average =	172	7.42	29.4	7.72	154	0.45	0.88	0.43	1.96	1.08
					stdev =	48	1.17	0.3	0.20	33	0.26	0.23	0.08	0.49	0.47
					n =	7	6	7	7	7	7	7	7	7	7

Appendix 2. Field and laboratory parameters for Mekong River sampling in Laos during October 24-25, 2012.

		Latitude	Longitude	River	Sampling	(µS/cm)	mg/L	°C		mg/L	(µM)	filtered		unfiltered		$*(NO_2+NO_3)$		
Sample	**Date**	**°N**	**°E**	**depth (m)**	**depth (m)**	**conductivity**	**DO**	**Temp**	**pH**	**SS**	**DIP**	**TDP**	**DOP**	**TP**	**PP**	**NH_4**	**$*NO_3$**	**DIN**
MK1S	24-Oct-12	15.276	105.803	4.1	1.0	297	6.77	28.5	7.81	98	0.68	0.75	0.06	0.93	0.19	2.61	29.02	31.63
MK1B	24-Oct-12				3.5	300	6.86	28.5	7.83	109	0.67	0.88	0.21	1.19	0.31	3.77	28.67	32.44
MK2S	24-Oct-12	15.067	105.834	12.7	1.0	309	6.82	28.6	7.83	107	0.70	0.76	0.06	0.90	0.14	4.30	28.31	32.61
MK2M	24-Oct-12				6.0	307	6.71	28.5	7.83	107	0.71	0.77	0.06	0.93	0.16	3.79	29.40	33.19
MK2B	24-Oct-12				12.0	307	6.85	28.5	7.83	107	0.67	0.80	0.12	1.01	0.21	18.32	28.40	46.72
MK3S	24-Oct-12	14.936	105.897	4.7	1.0	312	6.78	28.9	7.84	98	0.78	1.35	0.57	2.11	0.76	3.52	30.16	33.68
MK3B	24-Oct-12				4.0	311	6.78	28.9	7.83	101	0.78	0.80	0.02	1.10	0.29	2.78	31.13	33.91
MK4S	24-Oct-12	14.801	105.915	5.1	1.0	309	6.76	29.0	7.83	96	0.73	0.80	0.07	0.93	0.13	10.88	27.93	38.81
MK4B	24-Oct-12				4.5	309	6.71	29.0	7.84	100	0.80	0.82	0.01	1.05	0.23	3.75	28.24	31.99
MK5S	24-Oct-12	14.717	105.912	7.1	1.0	312	6.97	29.2	7.85	95	0.80	0.82	0.02	0.98	0.16	2.75	29.58	32.33
MK5M	24-Oct-12				3.0	312	6.92	29.2	7.90	96	0.82	0.85	0.03	0.87	0.01	2.72	29.00	31.71
MK5B	24-Oct-12				6.0	311	6.90	29.2	7.91	109	0.95	1.11	0.16	1.14	0.04	2.72	28.76	31.48
MK6S	24-Oct-12	14.661	105.878	7.0	1.0	309	6.91	29.2	7.88	90	0.78	0.94	0.15	1.09	0.15	2.99	29.69	32.67
MK6M	24-Oct-12				3.0	308	6.96	29.1	7.89	71	0.93	0.94	0.01	1.29	0.35	3.32	32.60	35.92
MK6B	24-Oct-12				6.0	308	7.00	29.1	7.89	93	0.81	0.95	0.14	1.65	0.71	3.69	28.27	31.96
MK7S	24-Oct-12	14.560	105.860	4.0	1.0	304	6.85	28.9	7.88	97	0.74	0.76	0.01	1.09	0.33	3.08	26.44	29.53
MK7B	24-Oct-12				3.0	305	6.98	28.9	7.88	98	0.79	0.82	0.03	1.03	0.21	3.87	26.98	30.85
MK8S	25-Oct-12	14.389	105.867	5.9	1.0	307	6.86	29.2	7.88	96	0.81	0.90	0.09	0.96	0.06	4.14	28.47	32.61
MK8B	25-Oct-12				5.0	308	6.81	29.2	7.89	100	1.05	1.18	0.13	1.42	0.24	5.06	27.71	32.77
MK9S	25-Oct-12	14.339	105.875	8.9	1.0	312	6.78	29.0	7.88	61	0.82	0.95	0.13	1.33	0.38	17.57	32.70	50.27
MK9M	25-Oct-12				4.0	312	6.77	29.0	7.89	88	0.94	1.04	0.10	1.44	0.40	16.91	32.34	49.25
MK9B	25-Oct-12				8.0	311	6.71	29.0	7.88	109	0.80	0.94	0.14	1.07	0.13	13.94	28.83	42.76
MK10S	25-Oct-12	14.227	105.849	8.8	1.0	308	6.87	29.0	7.92	83	0.85	0.96	0.11	1.21	0.25	16.71	33.48	50.19
MK10M	25-Oct-12				4.0	307	6.84	28.9	7.92	87	0.88	1.05	0.18	1.51	0.45	14.78	34.47	49.25
MK10B	25-Oct-12				8.0	306	6.89	28.9	7.91	93	0.82	0.93	0.11	0.98	0.05	13.90	33.68	47.57
MK11S	25-Oct-12	14.088	105.843	15.0	1.0	308	6.95	29.2	7.91	81	0.79	1.15	0.36	1.18	0.03	14.70	34.41	49.12
MK11M	25-Oct-12				7.0	307	6.91	29.1	7.91	89	0.85	0.99	0.15	1.61	0.62	12.44	34.93	47.37
MK11B	25-Oct-12				14.0	307	6.90	29.1	7.89	89	1.06	0.95	-0.11	1.14	0.19	11.71	37.23	48.94
MK12S	25-Oct-12	14.057	105.890	5.5	1.0	308	6.89	29.2	7.90	90	0.72	1.01	0.30	1.28	0.26	17.34	32.36	49.70
MK12B	25-Oct-12				4.5	307	6.89	29.2	7.88	90	0.84	1.00	0.16	1.62	0.63	19.29	30.51	49.80
MK13S	25-Oct-12	13.992	105.914		1.0	310	6.81	29.7	7.94	91	0.90	1.06	0.16	1.21	0.15	19.49	33.17	52.66
MK13B	25-Oct-12			8.3	7.0	310	6.80	29.8	7.92	93	0.82	1.10	0.28	1.14	0.04	20.98	42.29	63.27
					average =	308	6.85	29.0	7.88	94	0.82	0.94	0.13	1.20	0.26	9.31	30.91	40.22
					stdev =	3	0.08	0.3	0.03	11	0.10	0.14	0.12	0.27	0.20	6.66	3.39	9.17
					n =	32	32	32	32	32	32	32	32	32	32	32	32	32

Appendix 3. Field and laboratory parameters for Tonle Sap Lake sampling during January 20-23, 2013.

												filtered		unfiltered			*(NO_2+NO_3)		
Station	**Lat**	**Long**	**Date of Sampling**	**Water Depth**	**Sampling Depth**	**Conductivity**	**DO**	**Temp**	**pH**	**SS**	**DIP**	**TDP**	**DOP**	**TP**	**PP**	**NH_4**	**$*NO_3$**	**DIN**	**Chl-a**
				m	**m**	**uS/cm**	**mg/L**	**°C**		**mg/L**	**µM**	**µM**	**µM**	**µM**	**µM**	**µM**	**µM**	**µM**	mg/L
1	13° 14.876	103° 49.381	20-Jan-13	1.9	1.0	123	2.85	25.2	6.48	478	1.19	1.41	0.22	1.25	0.06	13.81	22.62	36.42	13.8
2	13° 13.987	103° 48.036	20-Jan-13	2.3	1.0	187	6.82	26.0	6.52	25	0.00	1.06	1.06	1.24	1.24	23.61	2.19	25.81	14.1
3	13° 14.383	103° 46.355	20-Jan-13	2.2	1.0	225	6.91	25.7	6.67	27	0.12	1.15	1.03	1.47	1.35	12.99	6.26	19.24	21.2
4	13° 14.063	103° 43.409	20-Jan-13	2.0	1.0	214	6.89	26.1	6.62	39	1.42	1.61	0.19	1.60	0.18	11.51	9.41	20.92	36.1
5	13° 13.878	103° 42.253	20-Jan-13	1.9	1.0	232	8.65	27.7	6.49	16	0.08	0.98	0.90	1.00	0.92	10.93	8.95	19.88	19.4
6	13° 14.089	103° 40.924	20-Jan-13	1.4	0.7	194	1.93	26.9	6.24	7	0.00	0.78	0.78	1.11	1.11	11.61	10.32	21.93	9.2
7	13° 12.928	103° 41.382	21-Jan-13	2.4	1.2	226	2.26	24.9	6.33	11	0.14	0.89	0.75	1.11	0.98	14.72	8.00	22.71	9.2
8	13° 11.975	103° 43.176	21-Jan-13	2.0	1.0	192	5.63	25.1	6.44	65	0.38	0.78	0.40	1.19	0.81	13.00	9.75	22.75	18.4
9	13° 10.428	103° 44.690	21-Jan-13	2.3	1.1	155	6.39	25.1	6.45	64	0.42	0.91	0.48	1.50	1.08	14.32	13.45	27.77	15.0
10	13° 08.811	103° 46.454	21-Jan-13	2.4	1.2	155	6.72	25.4	6.13	55	0.40	0.92	0.52	1.19	0.80	13.27	8.75	22.02	15.8
11	13° 06.709	103° 48.120	21-Jan-13	2.4	1.2	147	7.18	26.0	6.37	41	0.26	0.83	0.57	1.35	1.09	12.51	4.89	17.40	13.5
12	13° 04.923	103° 49.919	21-Jan-13	2.4	1.2	146	7.47	26.5	6.34	39	0.22	0.93	0.71	1.29	1.07	13.40	3.46	16.85	9.1
13	13° 03.225	103° 51.840	21-Jan-13	2.5	1.2	155	7.65	26.2	6.35	38	0.17	0.99	0.82	1.33	1.17	12.91	5.53	18.44	10.7
14	13° 13.066	103° 42.511	22-Jan-13	1.9	1.0	232	3.09	25.2	6.37	16	0.12	0.68	0.56	0.87	0.75	13.04	2.70	15.74	14.5
15	13° 12.382	103° 44.756	22-Jan-13	2.3	1.1	176	6.78	25.9	6.34	70	0.32	0.85	0.53	0.93	0.62	12.90	14.95	27.86	19.9
16	13° 11.712	103° 46.889	22-Jan-13	2 .3	1.1	165	7.09	26.0	6.29	79	0.86	0.88	0.01	1.31	0.45	22.75	12.81	35.56	16.2
17	13° 10.934	103° 49.064	22-Jan-13	2.6	1.3	164	6.98	26.3	6.29	56	0.61	1.14	0.52	1.25	0.64	15.43	11.40	26.83	12.0
18	13° 09.857	103° 51.469	22-Jan-13	2.4	1.2	169	8.02	26.6	6.25	56	0.63	0.77	0.13	1.30	0.66	13.30	9.24	22.54	16.1
19	13° 07.538	103° 52.695	22-Jan-13	2.7	1.3	166	8.79	26.3	6.28	26	0.11	0.80	0.69	1.09	0.98	13.10	6.56	19.66	24.0
20	13° 09.892	103° 53.082	22-Jan-13	2.6	1.3	176	8.57	27.4	6.26	38	0.29	0.42	0.13	0.95	0.66	14.02	10.10	24.12	20.3
21	13° 11.715	103° 51.683	22-Jan-13	2.6	1.3	192	8.03	27.3	6.53	58	0.28	0.93	0.65	1.05	0.77	15.52	11.38	26.90	18.9
22	13° 13.526	103° 49.945	22-Jan-13	2.3	1.1	178	9.25	28.7	6.23	54	0.18	0.76	0.59	0.83	0.65	12.85	4.70	17.55	58.9
23	13° 13.388	103° 50.845	22-Jan-13	2.0	1.0	168	7.35	28.0	6.21	41	0.70	0.96	0.25	1.05	0.35	14.05	4.10	18.15	32.6
24	13° 12.504	103° 52.910	23-Jan-13	2.3	1.1	188	8.59	27.6	6.33	59	0.16	0.74	0.58	1.29	1.13	13.61	3.64	17.25	72.4
25	13° 12.505	103° 55.082	23-Jan-13	2.0	1.0	177	8.00	28.0	6.33	37	0.25	1.08	0.83	1.23	0.98	11.13	6.09	17.22	36.4
26	13° 11.789	103° 57.766	23-Jan-13	2.2	1.1	168	7.61	28.3	6.31	58	0.30	0.81	0.52	1.20	0.90	13.28	16.21	29.49	56.2
27	13° 11.212	103° 59.626	23-Jan-13	2.0	1.0	169	7.54	28.5	6.24	29	0.52	0.54	0.02	0.90	0.37	12.96	21.55	34.52	23.9
28	13° 09.647	104° 01.522	23-Jan-13	2.2	1.1	164	7.30	28.7	6.35	21	0.53	0.64	0.10	1.00	0.47	13.52	21.61	35.13	13.0
29	13° 08.001	104° 03.017	23-Jan-13	2.0	1.0	167	7.97	28.9	6.30	17	0.30	0.54	0.24	1.45	1.15	13.38	14.93	28.31	19.2
					average =	178	6.84	26.7	6.36	56	0.38	0.89	0.51	1.18	0.81	13.91	9.85	23.76	22.8
					stdev =	27	1.93	1.2	0.12	83	0.33	0.25	0.29	0.20	0.33	2.78	5.65	6.16	15.6
					n =	29	29	29	29	29	29	29	29	29	29	29	29	29	29

Appendix 4. Field and laboratory parameters for Tonle Sap Lake sampling during July 14-18, 2013.

												filtered		unfiltered			$^*(NO_2+NO_3)$		
Station	**Lat**	**Long**	**Date of Sampling**	**Water Depth**	**Sampling Depth**	**Conductivity**	**DO**	**Temp**	**pH**	**SS**	**DIP**	**TDP**	**DOP**	**TP**	**PP**	**NH_4**	**$^*NO_3$**	**DIN**	**Chl-a**
				m	m	uS/cm	mg/L	°C		mg/L	µM	µM	µM	µM	µM	µM	µM	µM	mg/L
30	13°13.918′	103°42.666′	14-Jul-13	2.1	1.0	96	3.06	30.3	5.75	151	0.99	1.11	0.12	1.64	0.53	16.12	7.73	23.85	9.3
31	13°12.963′	103°47.758′	14-Jul-13	2.0	1.0	129	6.78	29.9	7.34	253	0.86	0.96	0.10	1.65	0.69	9.21	11.34	20.55	17.1
32	13°12.660′	103°45.686′	14-Jul-13	1.8	1.0	128	6.57	30.0	7.00	392	0.94	1.09	0.15	1.67	0.58	7.85	20.35	28.21	24.1
33	13°11.767′	103°44.920′	14-Jul-13	1.8	1.0	117	6.98	29.9	7.09	920	1.04	1.43	0.38	1.99	0.56	5.51	22.11	27.63	35.4
34	13°11.248′	103°47.290′	14-Jul-13	1.9	1.0	119	7.00	30.0	7.23	922	1.41	1.69	0.28	2.13	0.45	6.19	24.50	30.69	32.2
35	13°12.847′	103°49.104′	14-Jul-13	2.0	1.0	137	6.84	30.4	7.31	166	1.02	1.07	0.05	1.65	0.58	10.24	7.03	17.27	14.9
36	13°13.291′	103°50.135′	15-Jul-13	1.8	1.0	146	6.44	30.1	6.97	185	0.94	1.06	0.12	1.45	0.39	8.36	10.66	19.02	17.7
37	13°11.563′	103°52.166′	15-Jul-13	2.0	1.0	122	6.90	29.7	6.94	552	0.97	1.38	0.42	1.60	0.21	10.58	17.27	27.85	23.6
38	13°09.799′	103°53.816′	15-Jul-13	2.2	1.0	131	7.01	30.1	6.94	1134	1.91	2.02	0.11	2.53	0.51	5.93	16.93	22.86	35.1
39	13°08.077′	103°55.300′	15-Jul-13	2.4	1.0	127	6.95	30.1	7.03	1507	2.06	2.56	0.50	2.82	0.25	9.23	20.25	29.49	34.5
40	13°05.808′	103°56.298′	15-Jul-13	2.2	1.0	113	6.94	30.1	6.96	1584	1.71	2.51	0.80	2.50	0.00	9.48	20.45	29.93	33.4
41	13°07.552′	103°57.341′	15-Jul-13	2.4	1.0	124	6.85	30.3	6.95	1303	2.10	2.31	0.21	2.63	0.33	11.37	18.18	29.55	32.7
42	13°09.412′	103°58.150′	15-Jul-13	2.3	1.0	114	6.94	30.9	7.08	932	1.24	2.08	0.84	2.34	0.26	12.30	21.14	33.44	30.9
43	13°10.895′	103°58.639′	16-Jul-13	2.1	1.0	115	6.49	29.8	6.77	607	1.03	1.45	0.42	1.72	0.27	8.94	17.83	26.76	28.7
44	13°08.799′	103°59.034′	16-Jul-13	2.3	1.0	114	6.83	29.6	6.88	1000	1.27	2.48	1.21	3.11	0.63	8.34	22.68	31.02	39.3
45	13°06.938′	103°58.243′	16-Jul-13	2 .3	1.0	123	6.84	29.5	6.94	1428	2.16	2.55	0.39	2.62	0.07	12.59	18.14	30.74	32.8
46	13°04.471′	103°57.565′	16-Jul-13	2.4	1.0	120	6.70	29.7	6.81	1580	1.76	2.55	0.79	2.58	0.03	9.15	20.39	29.54	34.6
47	13°02.387′	103°57.329′	16-Jul-13	2.4	1.0	125	6.91	29.9	6.86	1168	1.40	1.81	0.41	2.41	0.60	6.32	19.29	25.61	32.0
48	13°04.041′	103°58.854′	16-Jul-13	2.5	1.0	112	7.08	30.0	6.78	1585	1.50	2.57	1.06	2.71	0.14	5.91	24.33	30.24	33.7
49	13°06.359′	104°01.938′	16-Jul-13	2.5	1.0	121	6.99	30.0	6.81	1015	1.53	2.10	0.57	2.25	0.15	6.37	18.40	24.77	31.6
50	13°03.525′	104°04.991′	17-Jul-13	1.8	1.0	132	6.74	28.4	6.73	1715	1.49	1.68	0.19	2.63	0.95	4.89	34.26	39.15	44.5
51	13°00.432′	104°05.082′	17-Jul-13	2.7	1.0	141	7.08	28.3	6.72	1120	1.36	1.84	0.48	1.89	0.05	8.12	29.01	37.13	35.7
52	12°58.027′	104°06.768′	17-Jul-13	1.8	1.0	123	7.14	28.5	6.70	1136	1.32	1.96	0.64	2.18	0.22	5.65	26.61	32.26	45.2
53	12°55.499′	104°07.690′	17-Jul-13	1.7	1.0	102	7.21	28.7	6.74	948	1.20	1.42	0.22	2.07	0.66	7.57	11.48	19.05	38.3
54	12°52.509′	104°09.006′	17-Jul-13	1.9	1.0	128	7.40	29.0	6.90	525	0.77	1.26	0.49	1.64	0.38	5.29	7.11	12.40	28.0
55	12°49.890′	104°10.350′	17-Jul-13	2.0	1.0	200	7.22	29.4	6.96	293	0.42	0.55	0.13	1.32	0.78	5.08	1.46	6.53	24.7
56	12°47.508′	104°11.699′	17-Jul-13	2.0	1.0	181	6.95	30.0	6.91	335	0.59	0.63	0.03	1.65	1.03	4.83	4.05	8.89	28.0
57	12°44.265′	104°13.803′	17-Jul-13	1.7	1.0	196	7.41	30.1	6.95		0.54	0.60	0.06	2.13	1.53	6.17	7.56	13.73	49.0
58	12°43.509′	104°15.219′	18-Jul-13	2.1	1.0	159	6.88	28.7	6.80	221	0.68	0.85	0.16	1.36	0.51	8.00	12.98	20.98	33.2
59	12°41.641′	104°15.292′	18-Jul-13	2.2	1.0	194	7.28	28.8	6.72	154	0.58	0.64	0.07	1.24	0.60	3.14	14.97	18.10	17.4
60	12°39.018′	104°14.861′	18-Jul-13	2.4	1.0	167	7.10	29.1	6.79	204	1.01	1.08	0.07	1.77	0.69	9.06	21.24	30.30	9.5
61	12°36.904′	104°13.828′	18-Jul-13	2.4	1.0	158	7.12	29.6	6.74		1.68	2.21	0.53	2.57	0.37	7.95	6.78	14.73	10.6
62	12°36.263′	104°13.494′	18-Jul-13	2.8	1.0	135	6.99	29.8	6.69	42	1.32	1.51	0.18	2.04	0.53	13.21	15.13	28.35	5.4
station 61 = MRC station					average =	135	6.84	29.7	6.87	809	1.24	1.61	0.37	2.08	0.47	8.15	16.72	24.87	28.6
					stdev =	27	0.71	0.6	0.26	530	0.46	0.65	0.31	0.49	0.32	2.83	7.51	7.84	10.8
					n =	33	33	33	33	31	33	33	33	33	33	33	33	33	33

Appendix 5. Field and laboratory parameters for Tonle Sap River sampling during September 17-18, 2013.

												filtered		unfiltered			*(NO_2+NO_3)		
Station	**Date of Sampling**	**Lat**	**Long**	**Water Depth**	**Sampling Depth**	**Conductivity**	**DO**	**Temp**	**pH**	**SS**	**DIP**	**TDP**	**DOP**	**TP**	**PP**	**NH_4**	***NO_3**	**DIN**	**Chl-a**
				m	m	uS/cm	mg/L	°C		mg/L	µM	µM	µM	µM	µM	µM	µM	µM	mg/L
62	17-Sep-13	11° 34′ 30.6″	104° 55′ 54.6″	16.3	1	141	4.82	29.5	6.71	16	0.68	0.72	0.05	1.01	0.28	5.77	14.41	20.18	1.3
					12	146	5.81	29.0	6.83	38	0.71	0.84	0.13	1.18	0.34	7.13	19.92	27.05	0.7
63	17-Sep-13	11° 34′ 22.4″	104° 57′ 00.8″	12.3	1	145	6.88	28.5	7.00	194	0.73	0.79	0.06	1.73	0.93	####	16.71	30.66	0.7
					11	147	6.90	28.5	7.03	195	0.66	0.73	0.07	1.27	0.55	6.15	20.83	26.98	0.4
64	17-Sep-13	11° 35′ 23.6″	104° 55′ 20.4″	22.3	1	149	4.48	29.6	6.97	20	0.70	0.86	0.17	1.13	0.26	4.21	14.48	18.70	1.3
					12	150	4.57	29.6	7.06	17	0.67	0.77	0.10	0.99	0.22	6.68	15.05	21.73	1.5
65	17-Sep-13	11° 37′ 57.0″	104° 54′ 30.7″	19.2	1	149	4.42	29.7	7.00	17	0.92	0.96	0.04	1.30	0.34	5.17	15.51	20.67	1.3
					12	149	4.39	29.7	7.08	45	0.74	0.78	0.04	1.01	0.23	4.12	15.65	19.76	1.6
66	17-Sep-13	11° 39′ 08.2″	104° 52′ 26.2″	14.5	1	148	4.52	29.7	6.98	15	0.64	0.66	0.02	0.96	0.30	4.03	13.91	17.94	2.8
					12	149	4.56	29.6	7.06	15	0.71	0.74	0.02	0.98	0.24	3.70	13.96	17.65	1.9
67	17-Sep-13	11° 41′ 23.0″	104° 51′ 00.6″	13.0	1	146	4.91	29.8	7.00	15	0.64	0.69	0.05	1.00	0.31	####	14.14	24.26	2.0
					12	148	4.55	29.7	7.05	14	0.58	0.70	0.12	0.98	0.29	8.58	13.66	22.24	1.3
68	17-Sep-13	11° 44′ 13.3″	104° 50′ 11.0″	17.6	1	145	4.96	29.6	7.15	13	0.60	0.63	0.03	0.98	0.35	####	13.23	27.65	1.5
					12	146	4.78	29.6	7.03	16	0.60	0.75	0.14	0.80	0.05	4.17	13.67	17.84	1.6
69	17-Sep-13	11° 47′ 20.9″	104° 49′ 31.7″	18.2	1	145	5.30	29.8	6.91	12	0.65	0.71	0.05	0.96	0.26	4.27	13.11	17.38	2.7
					12	147	4.98	29.5	6.95	11	0.62	0.65	0.03	0.92	0.26	11.80	13.36	25.16	1.5
70	18-Sep-13	11° 50′ 49.4″	104° 48′ 12.2″	19.7	1	148	4.74	29.4	6.93	14	0.52	0.65	0.13	1.00	0.35	####	13.18	26.70	2.1
					12	150	4.82	29.4	6.93	17	0.64	0.66	0.02	0.94	0.27	9.96	13.29	23.25	2.2
71	18-Sep-13	11° 53′ 12.4″	104° 47′ 29.2″	10.4	1	147	4.80	29.4	6.88	16	0.53	0.76	0.23	1.06	0.30	####	11.06	21.26	2.2
					9	149	4.72	29.4	7.06	18	0.49	0.84	0.34	1.03	0.19	####	13.02	23.57	1.9
72	18-Sep-13	11° 55′ 12.8″	104° 49′ 29.7″	11.2	1	144	4.63	29.5	6.87	13	0.66	0.68	0.02	1.07	0.39	####	11.18	27.75	1.8
					10	147	4.64	29.5	7.01	17	0.70	0.74	0.04	1.05	0.32	####	13.48	26.91	1.9
73	18-Sep-13	11° 58′ 06.2″	104° 49′ 57.0″	18.7	1	143	4.80	29.6	7.14	11	0.64	0.86	0.22	1.09	0.24	####	13.41	28.02	1.5
					12	146	4.71	29.5	7.04	11	0.58	0.77	0.19	1.16	0.38	7.86	13.42	21.29	1.2
74	18-Sep-13	11° 59′ 51.3″	104° 48′ 27.7″	10.6	1	144	4.99	29.7	7.03	10	0.61	0.64	0.03	0.93	0.29	8.22	12.70	20.92	2.1
					9	147	4.73	29.6	6.96	16	0.53	0.76	0.23	5.51	4.75	4.16	13.05	17.21	2.6
75	18-Sep-13	11° 58′ 28.4″	104° 47′ 20.2″	11.7	1	143	4.95	29.7	7.25	14	0.58	0.69	0.11	0.92	0.23	5.30	13.35	18.66	1.1
					10	146	4.67	29.5	7.30	13	0.66	0.77	0.11	1.15	0.38	7.32	14.83	22.14	1.6
76	18-Sep-13	11° 56′ 31.5″	104° 48′ 08.6″	12.4	1	144	4.69	29.6	7.32	13	0.69	0.69	0.00	1.18	0.49	6.82	13.29	20.11	1.7
					11.0	147	4.96	29.5	7.22	16	0.60	0.61	0.01	1.04	0.43	4.91	13.70	18.62	1.4
					average =	146	4.92	29.5	7.03	28	0.64	0.74	0.09	1.21	0.47	8.26	14.15	22.41	1.6
					stdev =	2	0.60	0.3	0.13	46	0.08	0.08	0.08	0.83	0.82	3.86	2.04	3.87	0.6
					n =	30	30	30	30	30	30	30	30	30	30	30	30	30	30

Appendix 6. Field and laboratory parameters for Tonle Sap River sampling during June 24-26, 2014.

												filtered		unfiltered			$*(NO_2+NO_3)$		
Station	**Lat**	**Long**	**Date of Sampling**	**Water Depth**	**Sampling Depth**	**Conductivity**	**DO**	**Temp**	**pH**	**SS**	**DIP**	**TDP**	**DOP**	**TP**	**PP**	**NH_4**	**$*NO_3$**	**DIN**	**Chl-a**
				m	**m**	**uS/cm**	**mg/L**	**°C**		**mg/L**	**µM**	**µM**	**µM**	**µM**	**µM**	**µM**	**µM**	**µM**	mg/L
77	13°15.836´	103°49.333´	24-Jun-14	0.8	0.4	95	6.29	29.2	5.59	866	0.58	0.71	0.13	1.84	1.12	39.40	22.43	61.83	8.0
78	13°14.433´	103°49.514´	24-Jun-14	1.0	0.5	75	6.44	29.2	6.06	654	0.45	0.71	0.27	2.21	1.50	20.72	10.41	31.13	7.6
79	13°13.871´	103°49.655´	24-Jun-14	0.7	0.4	180	5.48	28.9	6.77	606	0.38	0.63	0.25	2.27	1.64	17.89	17.61	35.50	30.5
80	13°12.887´	103°49.469´	24-Jun-14	0.7	0.4	118	6.73	29.3	6.59	2143	0.52	0.62	0.10	3.04	2.42	12.49	24.47	36.96	74.3
81	13°11.686´	103°49.644´	24-Jun-14	0.7	0.4	147	7.00	29.5	6.74	2056	1.06	1.23	0.17	4.24	3.01	14.41	6.39	20.80	60.3
82	13°10.276´	103°49.064´	24-Jun-14	0.7	0.4	151	7.02	29.4	6.81	2100	0.90	1.61	0.70	4.25	2.64	10.86	10.85	21.71	55.9
83	13°08.143´	103°48.415´	24-Jun-14	0.7	0.4	152	7.08	29.6	6.74	2127	1.32	2.18	0.86	4.32	2.14	9.29	17.90	27.19	53.3
84	13°14' 11.3"	103°49' 41.2"	25-Jun-14	0.7	0.4	90	5.31	28.5	6.21	856	0.52	1.09	0.57	3.11	2.02	13.22	24.69	37.90	12.2
85	13°14' 09.6"	103°49' 41.9"	25-Jun-14	0.7	0.4	86	5.33	28.6	6.12	1078	0.39	0.51	0.12	3.91	3.41	14.68	20.01	34.69	16.3
86	13°13' 13.4"	103°50' 22.2"	25-Jun-14	0.9	0.5	176	6.65	28.3	6.66	1498	0.63	0.76	0.13	3.22	2.46	13.03	26.55	39.58	46.2
87	13°12' 53.0"	103°52' 10.3"	25-Jun-14	0.9	0.5	143	6.42	28.8	6.61	1843	0.58	0.74	0.16	3.22	2.48	13.32	37.13	50.44	64.6
88	13°12' 18.5"	103°53' 47.2"	25-Jun-14	1.1	0.6	134	6.70	29.3	6.60	1858	0.77	0.80	0.03	3.13	2.33	12.20	27.94	40.15	61.7
89	13°11' 45.4"	103°56' 02.1"	25-Jun-14	1.1	0.6	128	6.68	28.5	6.64	1996	0.51	0.57	0.07	3.69	3.12	11.25	22.05	33.30	74.2
90	13°11' 18.9"	103°58' 14.7"	25-Jun-14	0.9	0.5	176	6.30	29.1	6.76	1562	0.50	0.92	0.42	3.19	2.27	11.37	33.51	44.88	71.3
91	13°15' 06.5"	103°49' 20.7"	26-Jun-14	1.7	1.0	144	4.83	27.2	5.29	208	0.24	0.44	0.20	2.42	1.97	13.80	14.16	27.96	6.6
92	13°14' 35.7"	103°49' 21.2"	26-Jun-14	1.3	0.8	152	5.24	27.5	5.52	464	0.58	0.99	0.41	2.75	1.76	17.42	11.88	29.30	7.5
93	13°14' 10.4"	103°49' 41.4"	26-Jun-14	0.9	0.5	112	4.81	27.8	5.80	1133	0.26	0.74	0.48	2.61	1.87	22.92	27.43	50.35	12.8
94	13°13' 58.3"	103°49' 39.7"	26-Jun-14	0.9	0.5	111	4.13	27.6	5.99	1807	0.52	0.69	0.17	3.63	2.94	21.89	13.82	35.70	21.6
95	13°13' 47.4"	103°49' 38.7"	26-Jun-14	1.5	0.8	196	4.08	26.9	6.58	643	0.57	0.60	0.03	2.20	1.60	22.95	16.70	39.65	26.7
96	13°13' 21.0"	103°48' 41.1"	26-Jun-14	1.0	0.5	137	6.80	27.0	6.75	1904	0.49	0.71	0.22	3.23	2.52	18.67	29.48	48.15	56.8
97	13°13' 16.8"	103°47' 08.1"	26-Jun-14	1.0	0.5	141	6.73	27.3	6.72	1650	0.52	0.70	0.18	3.05	2.35	11.68	20.08	31.76	59.4
98	13°13' 15.0"	103°45' 43.6"	26-Jun-14	1.0	0.5	148	6.75	27.6	6.87	1330	0.65	0.89	0.25	2.96	2.07	12.79	29.05	41.84	52.7
99	13°12' 24.1"	103°44' 00.8"	26-Jun-14	0.9	0.5	137	6.48	27.9	6.70	1541	0.90	0.99	0.10	3.20	2.21	12.48	42.29	54.77	59.9
100	13°12' 30.8"	103°42' 46.3"	26-Jun-14	0.8	0.4	149	4.21	29.3	6.62	80	0.46	0.55	0.09	1.68	1.13	14.48	6.18	20.66	4.6
					average =	136	5.98	28.4	6.41	1333	0.60	0.85	0.25	3.06	2.21	15.97	21.38	37.34	39.4
					stdev =	31	0.99	0.9	0.46	651	0.24	0.38	0.22	0.73	0.59	6.37	9.38	10.65	25.3
					n =	24	24	24	24	24	24	24	24	24	24	24	24	24	24

Appendix 7. Field and laboratory parameters for Tonle Sap Lake sampling during November 7-10, 2014.

												filtered		unfiltered			$^*(NO_2+NO_3)$		
Station	**Lat**	**Long**	**Date of Sampling**	**Water Depth**	**Sampling Depth**	**Conductivity**	**DO**	**Temp**	**pH**	**SS**	**DIP**	**TDP**	**DOP**	**TP**	**PP**	**NH_4**	**$^*NO_3$**	**DIN**	**Chl-a**
				m	m	uS/cm	mg/L	°C		mg/L	µM	µM	µM	µM	µM	µM	µM	µM	mg/L
101	13°14.16′	103°49.68′	7-Nov-14	6.0	1	136	4.67	31.4	6.30	11	0.43	0.85	0.42	1.29	0.44	10.41	4.37	14.79	31.3
101	13°14.16′	103°49.68′	7-Nov-14	6.0	5	154	1.10	30.8	6.23	29	0.30	1.10	0.80	1.73	0.64	12.30	4.36	16.65	5.6
102	13°14.16′	103°49.68′	7-Nov-14	6.1	1	173	4.23	31.5	6.27	11	0.31	0.64	0.33	1.38	0.73	13.41	3.90	17.31	11.1
102	13°14.16′	103°49.68′	7-Nov-14	6.1	5	195	1.92	30.6	6.13	146	0.35	1.03	0.68	1.65	0.62	14.45	3.67	18.13	14.8
103	13°14.16′	103°49.68′	8-Nov-14	6.0	1	193	4.30	31.2	6.56	10	0.29	0.75	0.47	1.28	0.53	13.88	4.48	18.36	10.2
103	13°14.16′	103°49.68′	8-Nov-14	6.0	5	173	1.67	30.3	6.52	32	0.40	0.90	0.49	1.43	0.53	14.58	5.32	19.89	6.8
104	13°12.745′	103°49.873′	8-Nov-14	6.3	1	207	4.18	30.9	6.65	9	0.24	0.67	0.42	1.27	0.60	13.03	3.39	16.42	14.3
104	13°12.745′	103°49.873′	8-Nov-14	6.3	5	206	3.94	30.8	6.70	10	0.27	1.06	0.79	1.38	0.32	14.20	4.24	18.44	11.7
105	13°12.200′	103°51.681′	8-Nov-14	7.0	1	203	5.26	31.2	6.62	7	0.21	0.96	0.74	1.20	0.24	13.91	2.57	16.48	17.6
105	13°12.200′	103°51.681′	8-Nov-14	7.0	6	207	4.61	30.8	6.84	11	0.27	0.99	0.73	1.40	0.41	14.63	0.25	14.88	11.1
106	13°11.935′	103°53.413′	8-Nov-14	7.0	1	209	6.68	31.3	6.79	9	0.23	1.33	1.10	1.77	0.44	12.70	1.51	14.20	27.2
106	13°11.935′	103°53.413′	8-Nov-14	7.0	6	208	5.02	30.8	6.97	47	0.30	0.82	0.53	1.31	0.49	12.82	3.78	16.60	16.2
107	13°11.584′	103°56.084′	8-Nov-14	6.3	1	205	6.41	32.0	6.66	8	1.09	1.50	0.41	1.61	0.11	16.14	4.75	20.89	21.7
107	13°11.584′	103°56.084′	8-Nov-14	6.3	5	203	4.51	31.1	6.83	16	0.30	0.79	0.49	1.34	0.55	11.30	3.80	15.11	9.8
108	13°12.837′	103°58.452′	8-Nov-14	4.4	1	186	1.52	31.1	6.31	8	0.19	0.63	0.44	1.04	0.41	12.98	1.57	14.55	32.9
108	13°12.837′	103°58.452′	8-Nov-14	4.4	3	184	0.73	30.8	6.32	5	0.24	0.63	0.39	1.13	0.50	17.27	2.09	19.36	23.1
109	13°13.623′	103°51.038′	9-Nov-14	6.1	1	176	3.48	31.1	6.43	20	0.38	0.76	0.38	1.79	1.03	13.08	3.04	16.12	18.0
109	13°13.623′	103°51.038′	9-Nov-14	6.1	5	175	3.00	31.1	6.51	50	0.32	1.10	0.78	1.43	0.33	13.32	2.49	15.81	25.3
110	13°12.675′	103°54.493′	9-Nov-14	5.9	1	182	4.20	31.6	6.40	14	0.26	0.91	0.64	1.36	0.45	12.10	2.63	14.73	29.5
110	13°12.675′	103°54.493′	9-Nov-14	5.9	5	182	2.31	31.2	6.64	36	0.27	1.21	0.93	1.62	0.41	16.74	7.38	24.11	17.4
111	13°11.703′	103°58.027′	9-Nov-14	5.7	1	183	5.98	31.9	6.49	22	0.24	0.95	0.71	1.45	0.50	14.73	5.53	20.26	24.6
111	13°11.703′	103°58.027′	9-Nov-14	5.7	5	177	2.29	31.2	6.55	34	0.36	1.10	0.74	1.83	0.73	15.15	3.12	18.27	20.6
112	13°13.230′	103°58.485′	9-Nov-14	6.5	1	155	3.29	31.3	6.23	4	0.22	0.76	0.54	1.23	0.47	6.13	1.26	7.39	28.0
112	13°13.230′	103°58.485′	9-Nov-14	6.5	5	152	0.52	30.5	6.24	4	0.33	0.81	0.48	1.26	0.45	3.94	1.78	5.72	11.7
113	13°13.190′	103°58.474′	10-Nov-14	1.4	1	149	2.14	30.9	6.19	6	0.28	0.81	0.53	1.48	0.67	3.87	1.32	5.19	31.2
114	13°11.195′	103°58.222′	10-Nov-14	6.3	1	170	5.93	31.8	6.48	11	0.25	1.08	0.83	1.70	0.62	4.65	2.40	7.05	28.3
114	13°11.195′	103°58.222′	10-Nov-14	6.3	5	169	4.56	31.0	6.72	12	0.26	0.64	0.38	1.15	0.51	3.76	3.20	6.97	11.0
115	13°09.021′	103°57.292′	10-Nov-14	6.4	1	173	7.96	31.4	6.51	9	0.24	1.06	0.83	1.14	0.08	3.87	1.23	5.11	12.0
115	13°09.021′	103°57.292′	10-Nov-14	6.4	5	169	6.49	30.5	6.76	13	0.21	0.70	0.48	1.47	0.77	5.86	1.15	7.00	14.2
116	13°08.847′	103°56.112′	10-Nov-14	6.4	1	170	8.25	31.2	6.63	9	0.25	0.96	0.71	1.18	0.22	4.37	1.21	5.58	10.6
116	13°08.847′	103°56.112′	10-Nov-14	6.4	5	164	6.72	30.5	6.94	14	0.30	0.83	0.53	1.12	0.29	3.81	2.35	6.16	11.2
117	13°10.518′	103°54.169′	10-Nov-14	6.2	1	171	8.50	31.8	6.61	10	0.19	0.75	0.56	1.39	0.64	3.87	1.20	5.07	15.5
117	13°10.518′	103°54.169′	10-Nov-14	6.2	5	165	6.04	30.5	6.96	15	0.23	0.74	0.50	1.11	0.37	4.18	1.28	5.46	15.3
118	13°12.148′	103°52.034′	10-Nov-14	6.1	1	173	7.20	32.1	6.60	9	1.18	1.56	0.38	1.60	0.04	3.95	1.16	5.10	19.2
118	13°12.148′	103°52.034′	10-Nov-14	6.1	5	169	3.44	30.6	6.78	17	0.32	0.87	0.54	1.49	0.62	5.05	2.59	7.64	9.2
119	13°13.529′	103°50.366′	10-Nov-14	6.0	1	164	4.56	32.3	6.57	19	0.27	0.68	0.41	1.55	0.87	5.26	2.06	7.32	23.1
119	13°13.529′	103°50.366′	10-Nov-14	6.0	5	155	1.23	30.9	6.66	552	0.37	0.98	0.60	3.68	2.70	9.12	5.00	14.12	93.8
					average =	178	4.29	31.1	6.56	34	0.33	0.92	0.59	1.47	0.55	10.13	2.90	13.03	19.9
					stdev =	19	2.17	0.5	0.23	91	0.20	0.23	0.18	0.43	0.42	4.74	1.58	5.79	14.6
					n =	37	37	37	37	37	37	37	37	37	37	37	37	37	37

Appendix 8

Mass Balance Model of TS Phosphorus

ARCP2012-17NMY-Burnett

Submitted by

Veasna Kum

February 29, 2015

Contents

SYSTEM DYNAMICS MODELING OF PHOSPHORUS DYNAMICS IN TONLE SAP LAKE

1. General concepts on transport and loading

One of the basic processes in a lake (and most other surface waters) is the inflow and outflow of water with dissolved and particulate substances. The following mass balance is kept for each component in the water column:

$$\frac{dM}{dt} = c_{in}q_{in} - c_{out}q_{out} \tag{1}$$

$$\frac{dM}{dt} = \frac{dCV}{dt} = C\frac{dV}{dt} + V\frac{dC}{dt} \tag{2}$$

$$\frac{dV}{dt} = q_{in} - q_{out} \tag{3}$$

$$\frac{dC}{dt} = \frac{1}{V}\left(\frac{dM}{dt} - C\frac{dV}{dt}\right) \tag{4}$$

$$\frac{dC}{dt} = \frac{1}{V}\left[\left(c_{in}q_{in} - c_{out}q_{out}\right) - C\left(q_{in} - q_{out}\right)\right] \tag{5}$$

$$\frac{dC}{dt} = \frac{1}{V}\left[q_{in}\left(c_{in} - C\right) - q_{out}\left(c_{out} - C\right)\right] \tag{6}$$

As c_{out} equals C for all outflows except evaporation (where the outflow concentration is zero), the differential equation for concentration reduces to

$$\frac{dC}{dt} = \frac{1}{V}\left[q_{in}\left(c_{in} - C\right) - q_{evap}\left(0 - C\right)\right] \tag{7}$$

$$\frac{dC}{dt} = \frac{1}{V}\left[q_{in}c_{in} - q_{in}C + q_{evap}C\right] \tag{8}$$

$$\frac{dC}{dt} = \frac{1}{V}\left[\left(c_{in}q_{in}\right) - C\left(q_{in} - q_{evap}\right)\right] \tag{9}$$

Where

q_{in} : Sum of all water inflows to the lake
q_{out} : Sum of all water outflows from the lake
q_{evap} : Evaporation as outflow from the lake
c_{in} : Concentration of the component in those inflows
c_{out} : Concentration of the component in the lake
C : Concentration of the component in the lake
V : Volume of the lake

2. System dynamics modeling of phosphorus in the Lake

Structure of the phosphorus model

Phosphorus dynamics in the lake is dependent on the inflow and outflow of phosphorus and the loss and release to/from the sediments. Figure 1 and Figure 2 show stock and flow diagrams (SFD) of the model that illustrates the seasonal change of volume of the lake and the principal inputs and outputs of P that are considered in our model. For the present case, the form of phosphorus being considered includes particulate and dissolved forms of P. The model developed to study the behavioral dynamics of P in the water column seems reasonable in term of balancing the complexity and reality. The list of all variables of the model with description is shown in Table 1.

The structure of the P model for the lake Tonle Sap as presented in this report has been designed and redesigned many times to reasonably balance the complexity of the dynamic complexity of the lake and the data deficiency. The P model was developed, calibrated and tested. The P model was built in Vensim, a software program that facilitates one to conceptualize, document, simulate, analyze and optimize models of dynamic systems.

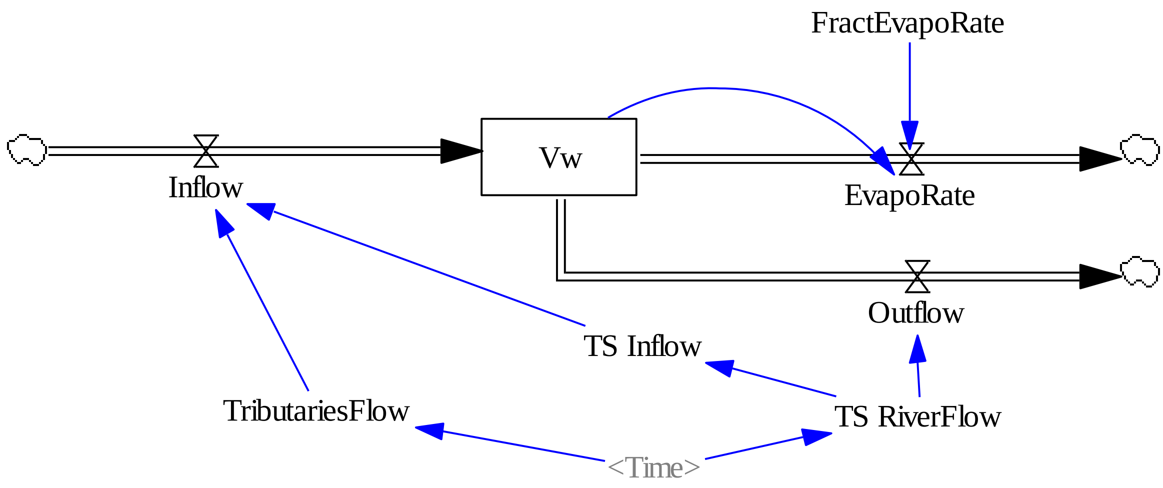

Figure 1: SFD of the lake volume showing inflow and outflow into and from the lake

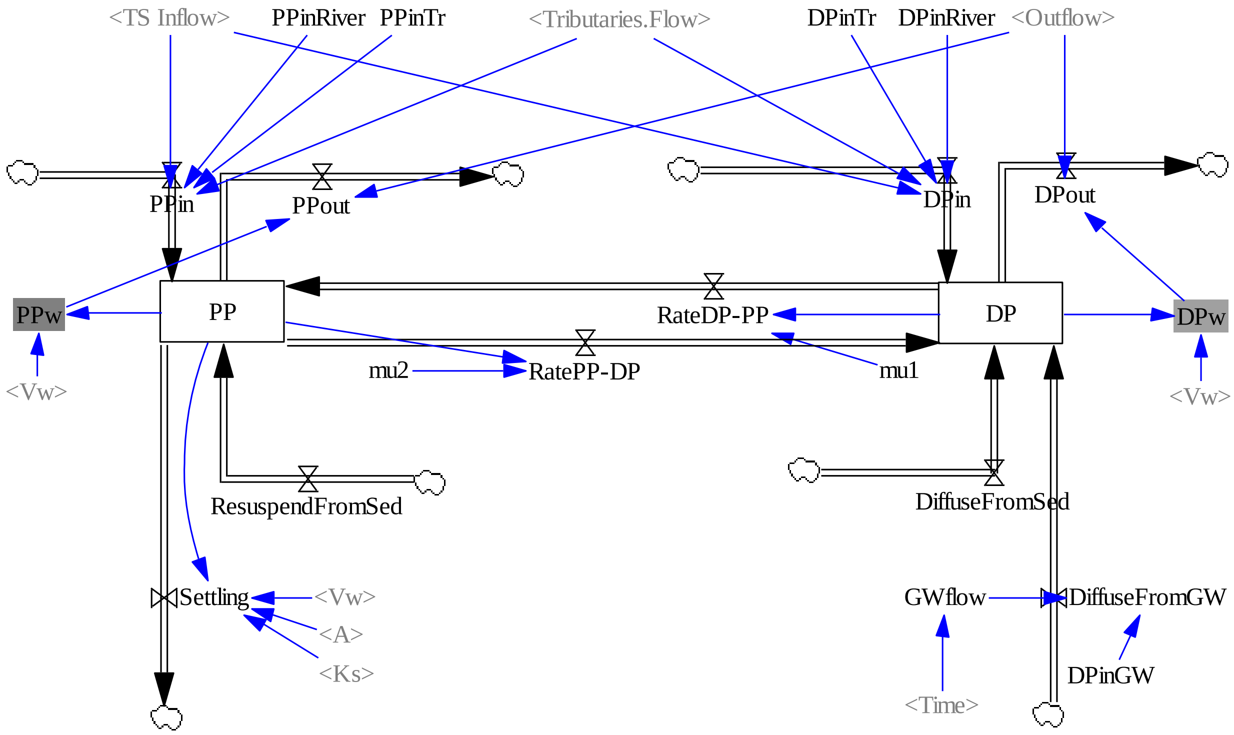

Figure 2: SFD of the model showing major inputs and outputs into and from the lake

Table 1: List of variables and parameters of the P model

Variable	*Description*	*Unit*
Vw	Seasonal volume of the lake	km3
A	Seasonal surface area of the lake	km2
Inflow	Rate of total flow of water into the lake	km3/month
TS Inflow	Rate of water flow of Tonle Sap river only into the lake	km3/month
TS RiverFlow	Rate of water flow of Tonle Sap river at Kompong Luang	km3/month
TributariesFlow	Rate of flow of water into the lake from the tributaries	km3/month
Outflow	Rate of water flow from the lake back to the river	km3/month
EvapoRate	Rate of flow of water out from the lake due to evaporation	km3/month
FracEvapoRate	Fractional rate of evaporation	1/month
PPin	Particulate phosphorus entering the lake	mg P/l/month
PPinRiver	Concentration of PP in Tonle Sap river	mg P/l
PPinTr	Concentration of PP in tributaries	mg P/l
DPin	Dissolved phosphorus entering the lake	mg P/l/month
DPinRiver	Concentration of DP in Tonle Sap river	mg P/l
DPinTr	Concentration of DP in tributaries	mg P/l
PPout	Particulate phosphorus exiting from the lake	tonne/month
DPout	Dissolved phosphorus exiting from the lake	tonne/month
ResuspendFromSed	Rate of resuspension of PP from the sediment	tonne/month
DiffuseFromSed	Rate of diffusion of DP from sediment	tonne/month
Settling	Rate of settling of PP to the sediment	tonne/month
GWflow	Rate of flow of groundwater to the lake	km3/month
DiffuseFromGW	Rate of diffusion of DP from the sediment	tonne/month

DPinGW	Concentration of DP in ground water	mg P/l
RateDP-PP	Rate of conversion from DP to PP in water column	tonne/month
RatePP-DP	Rate of conversion from PP to DP in water column	tonne/month
Mu1	Fractional rate of conversion from DP to PP	1/month
Mu2	Fractional rate of conversion from PP to DP	1/month
Ks	Velocity of settling of PP to the sediment	m/month
PP	Amount of total particulate phosphorus in water column	tonne
DP	Amount of total dissolved phosphorus in water column	tonne
PPw	Concentration of PP in the water column	mg P/l
DPw	Concentration of DP in the water column	mg P/l
h	Fitting constant to the function of TS RiverFlow	dimensionless
d	Fitting constant to the function of TS RiverFlow	month
a	Fitting constant to the function of TS RiverFlow	km3/month
c	Fitting constant to the function of TS RiverFlow	km3/month
k	Fitting constant to the function of TS RiverFlow	dimensionless

Observed behavior of PP and DP in the water column in 2001 and 2013

During 2001-2002, some researchers of Water and Development Research Group (WDRG) at Aalto University, Finland came to Cambodia and had conducted research in attempt to understand the impact of climate change and hydropower dam construction in the Mekong River on the Tonle Sap flood pulse. They did an excellent job collecting a large amount of hydrological and limnological data and some of them are shown here in **Table 2**. 12 years later, in 2013, our research work funded by APN collected data of similar type. The data shared by WDRG were used as a basis for comparison of behavior of lake phosphorus in 2001 and 2013 as shown in **Figure 3 and 4**. As seen in these figures, general behavior of particulate P does not change much between 2001 and 2013 except the peak in May which is lower. However, the behavior of dissolved P shows no specific pattern. Month 0 in **Figure 3 and 4** corresponds to January of years 2001 or 2013, respectively.

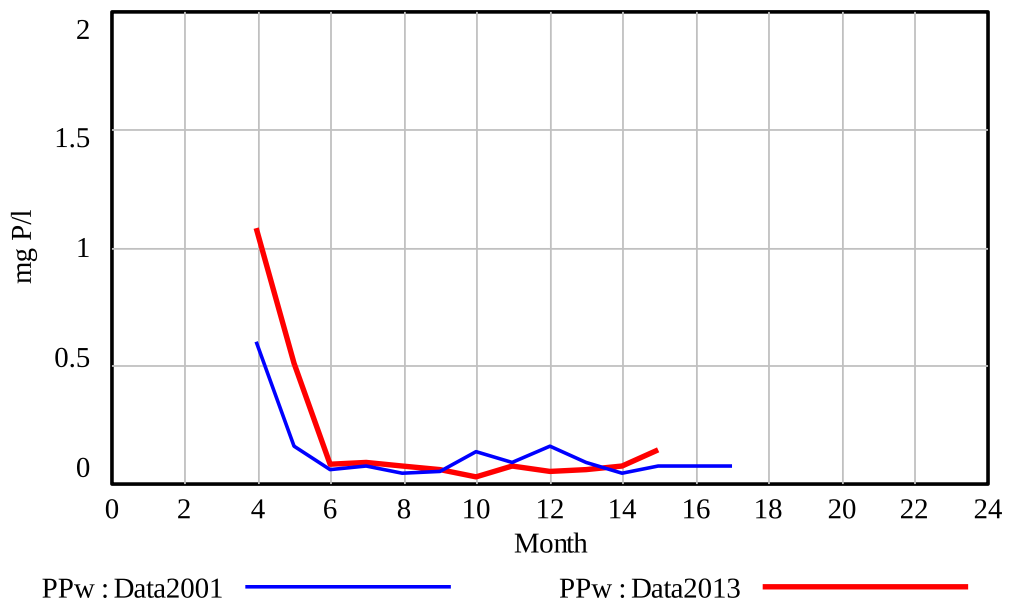

Figure 3: Observed behavior of particulate P in water column (PPw) in 2001 and 2013

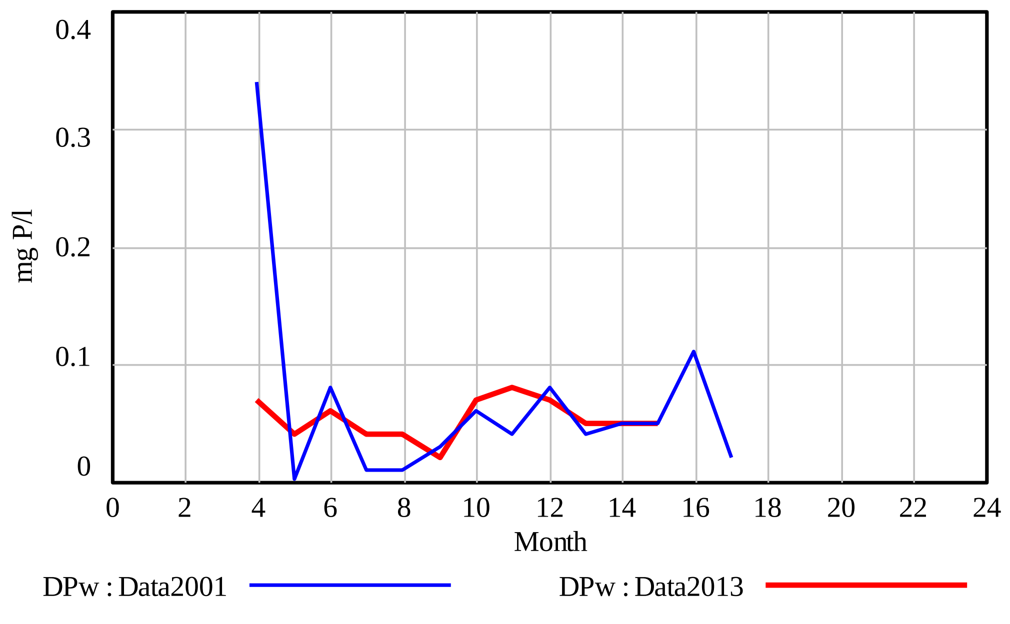

Figure 4: Observed behavior of dissolved P in water column (DPw) in 2001 and 2013

Table 2: Seasonal particulate and dissolved P of the lake in 2001&2013

Point#	Date	PPw--2001*	PPw--2013	DPw--2001*	DPw--2013

0	January	--	--	--	--
1	February	--	--	--	--
2	March	--	--	--	--
3	April	--	--	--	--
4	May	0.60	1.08	0.34	0.07
5	June	0.16	0.51	0.002	0.04
6	July	0.06	0.08	0.08	0.06
7	August	0.07	0.09	0.01	0.04
8	September	0.04	0.07	0.01	0.04
9	October	0.05	0.06	0.03	0.02
10	November	0.13	0.03	0.06	0.07
11	December	0.09	0.07	0.04	0.08
12	January	0.16	0.05	0.08	0.07
13	February	0.09	0.06	0.04	0.05
14	March	0.04	0.07	0.05	0.05
15	April	0.07	0.14	0.05	0.05

Source: * Personal communication with Dr. Matti Kummu

Estimates of water discharge rate and lake volume in 2001 and 2013

This section provides a comparison of the discharge rate to/from the lake and the corresponding seasonal volume of the lake in year 2001 and 2013. As seen in **Figure 5 and Figure 6**, the behavior of the discharge rate in 2001 and 2013 are basically the same but the peak in 2013 is a bit higher than that in 2001 and it is about two-months lag behind (the peak of the discharge rate in 2001 is in August but that in 2013 is in October). Similarly, the behavior of seasonal volume of the lake changes in a way that the volume in 2001 starts to increase in May but the volume in 2013 starts to increase in June. Month 0 in **Figure 5 and Figure 6** corresponds to January of years 2001 or 2013, respectively. The estimates of the discharge rate and the volume over time in 2001 and 2013 are shown in **Table 3 and Table 4**.

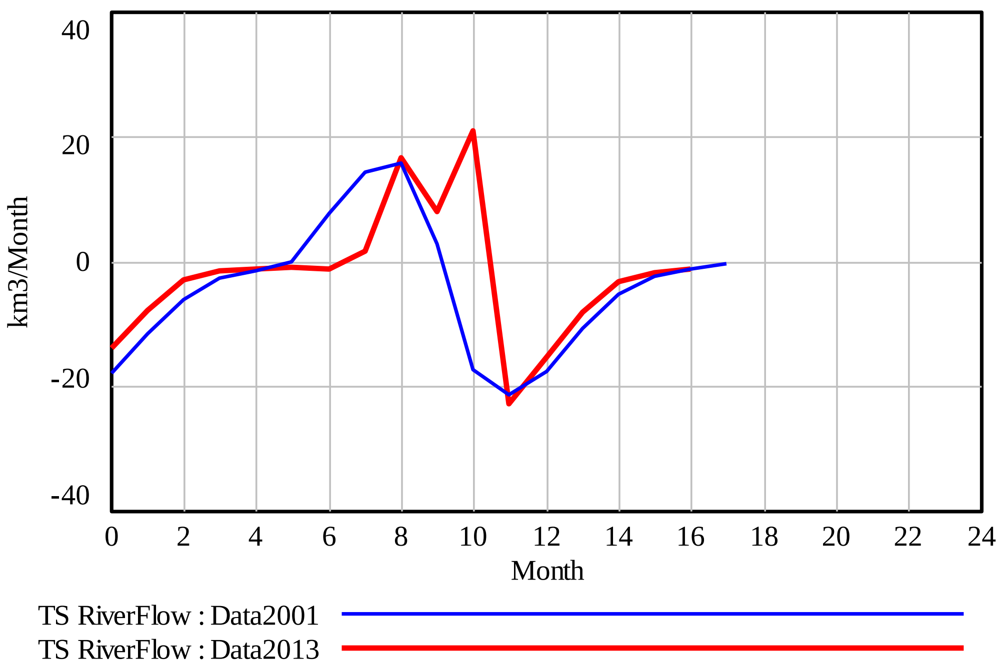

Figure 5: Seasonal water flow rate from/to the lake in 2001 and 2013

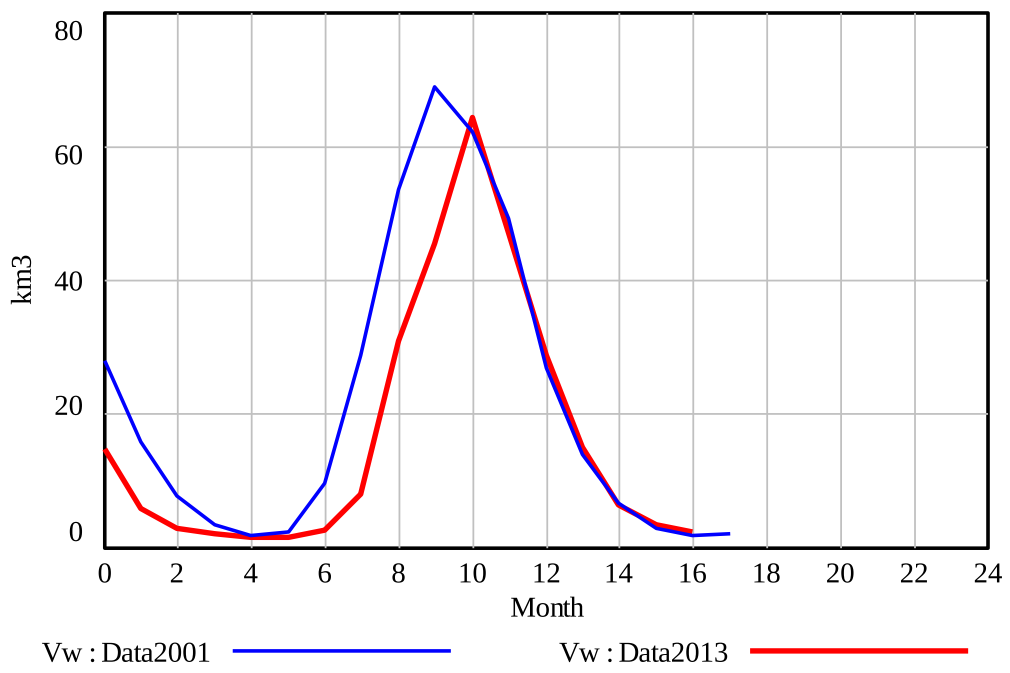

Figure 6: Seasonal volume of the lake in 2001 and 2013

Table 3: Seasonal water flow (km3/mo) into/from the Lake in 2001 & 2013

Point#	Date	TS RiverFlow—2001*	TS RiverFlow--2013

0	January	-18.00	-13.97
1	February	-11.60	-8.03
2	March	-6.10	-3.07
3	April	-2.86	-1.71
4	May	-1.52	-1.43
5	June	-0.28	-1.02
6	July	7.51	-1.38
7	August	14.10	1.45
8	September	15.60	16.49
9	October	2.77	7.82
10	November	-17.40	20.72
11	December	-21.40	-22.93
12	January	-17.60	-15.33
13	February	-10.70	-8.18
14	March	-5.34	-3.22
15	April	-2.44	-1.87

*Source: Personal communication with Dr. Matti Kummu

Table 4: Seasonal volume of the lake in 2001 & 2013

Point#	Date	Vw—2001*	Vw--2013
0	January	27.78	14.68
1	February	15.66	5.76
2	March	7.63	2.76
3	April	3.48	2.02
4	May	1.83	1.58
5	June	2.23	1.55
6	July	9.5	2.44
7	August	28.68	7.83
8	September	53.4	30.96
9	October	68.94	45.4
10	November	62.19	64.16
11	December	49.14	47.01
12	January	26.9	28.75
13	February	13.98	15.06
14	March	6.54	6.34
15	April	2.94	3.24

*Source: Personal communication with Dr. Matti Kummu

3. Calibration of the model

Calibration in SD modeling is also a part of model validation. The optimization tool in Vensim can be performed to calibrate a model. The powerful automate calibration tool of Vensim facilitates greatly the calibration work because manual calibration is not effective.

The list of parameters is shown in **Table 5**. We first calibrated the model to the data on water discharge to/from the lake and the seasonal volume of the lake. We found the behavior of these variables of the model fit very well to the data. Calibrated values from the calibration are assumed to be constant while performing the test of the impact of changing the discharge rate on the dynamics of particulate and dissolved P in the lake.

Table 5: List of model parameter values

Parameters	Values	Unit	References
FracEvapoRate	0.06	1/month	Calibrated in this study
ResuspendFromSed	20	tonne/month	Estimate in this study
DiffuseFromSed	5.5	tonne/month	Estimate in this study
Mu1	5	1/month	Calibrated in this study
	0.01-1.2	1/day	Lung (1976)
	0.06-2	1/day	Imboden (1974)
	0.06-2	1/day	Snodgrass&O'Melia (1975)
Mu2	0.5	1/month	Calibrated in this study
	0.001-0.12	1/day	Lung (1976)
	0.003-0.002	1/day	Imboden (1974)
	0.03	1/day	Snodgrass&O'Melia (1975)
Ks	4.5	m/month	Calibrated in this study
	0.3-0.5	m/day	Lung (1976)
	0.1-0.4	m/day	Imboden (1974)
	0.1-0.27	m/day	Snodgrass&O'Melia (1975)
h	1.14	dmnl	Calibrated to flow in 2001
	2.91	dmnl	Calibrated to flow in 2013
d	6.28	month	Calibrated to flow in 2001
	7.5	month	Calibrated to flow in 2013
a	17.93	km3/month	Calibrated to flow in 2001
	18.31	km3/month	Calibrated to flow in 2013
c	-0.33	km3/month	Calibrated to flow in 2001
	-0.33	km3/month	Calibrated to flow in 2013
k	-0.59	dmnl	Calibrated to flow in 2001
	-0.59	dmnl	Calibrated to flow in 2013

Calibrating water discharge in 2001

We proposed a function (10) to represent the dynamic discharge rate and this function is fitted to the data of water flow rate in 2001. As seen in **Figure 7**, the behavior of the water flow rate was successfully calibrated with *h*=1.14, *d*=6.28, *a*= 17.98, *c*= -0.33 and *k*= -0.59 (see **Table 5**).

$$f = \left[a\frac{Cos2\pi(t-d)}{12} + c\right]e^{h\frac{Sin2\pi(t-d)}{12}+k} \qquad (10)$$

where : *t* is time
a, c, d, h, k are all fitting constants

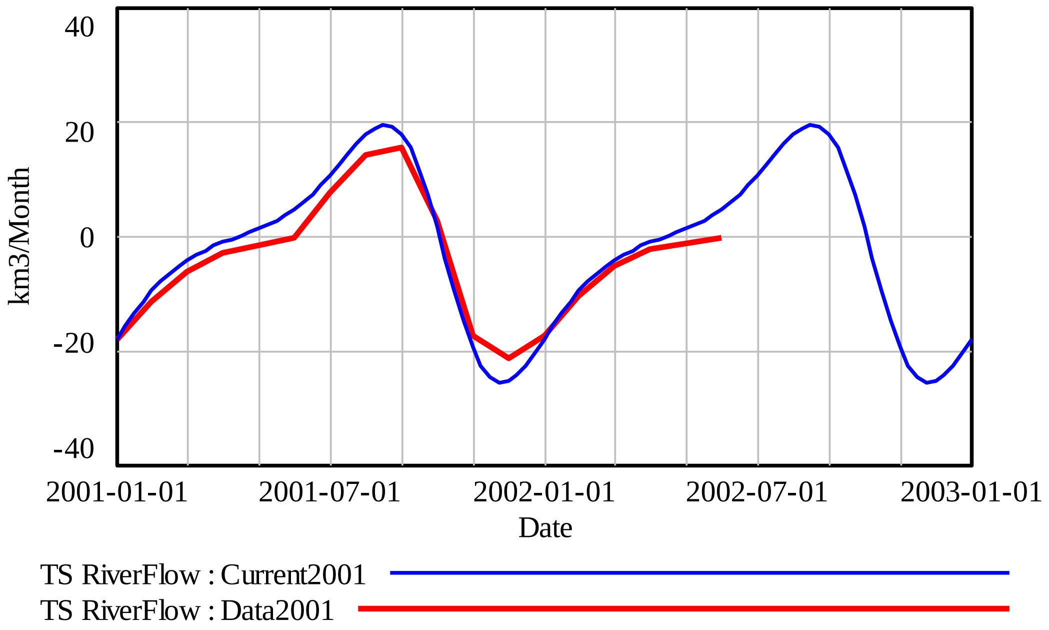

Figure 7: Calibrated water flow rate in 2001

Calibrating water volume in 2001

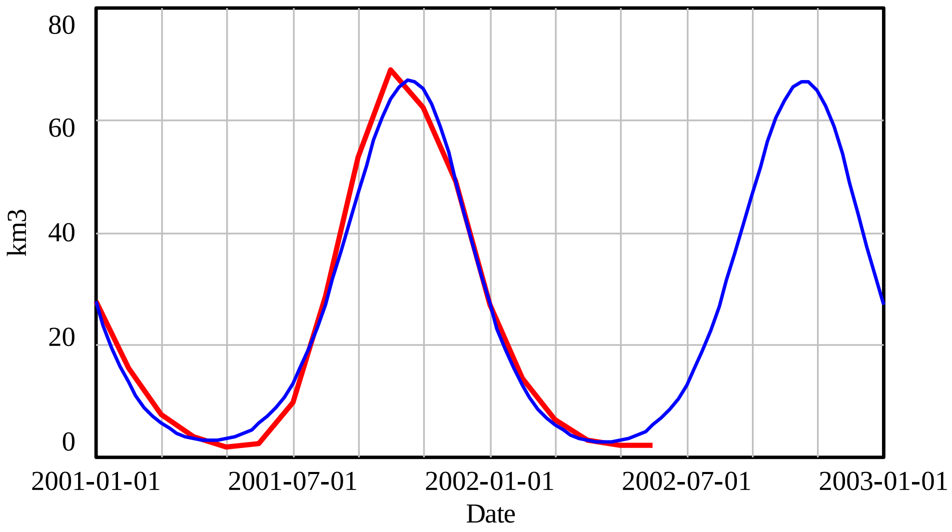

Figure 8: Calibrated seasonal water volume of the lake in 2001

Calibrating water discharge in 2013

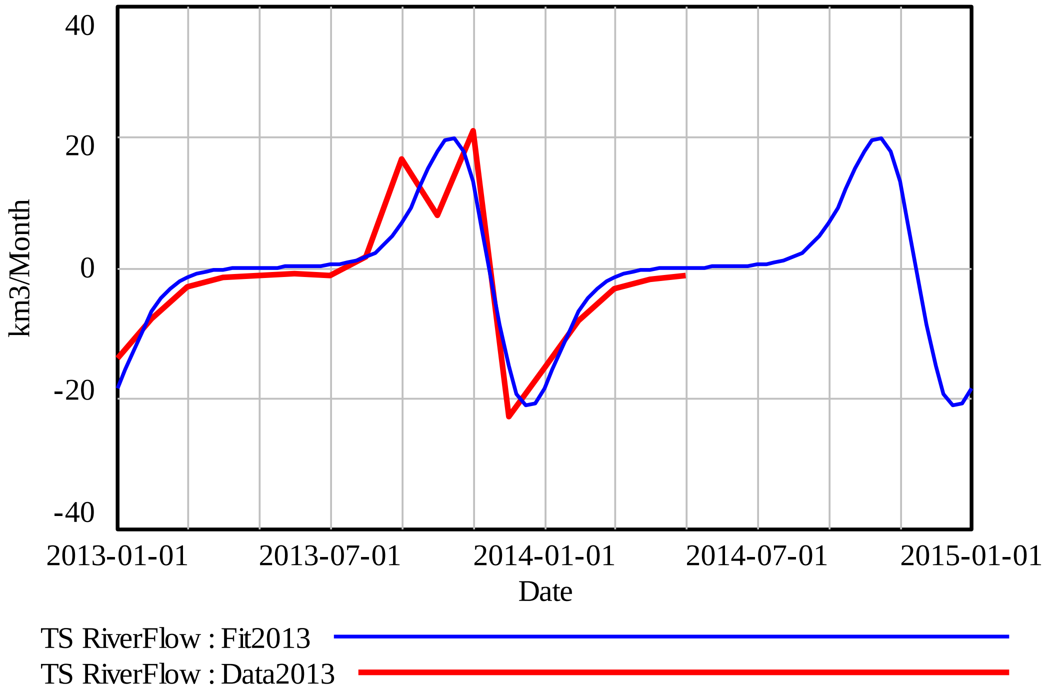

Figure 9: Calibrated water flow rate in 2013

Calibrating water volume in 2013

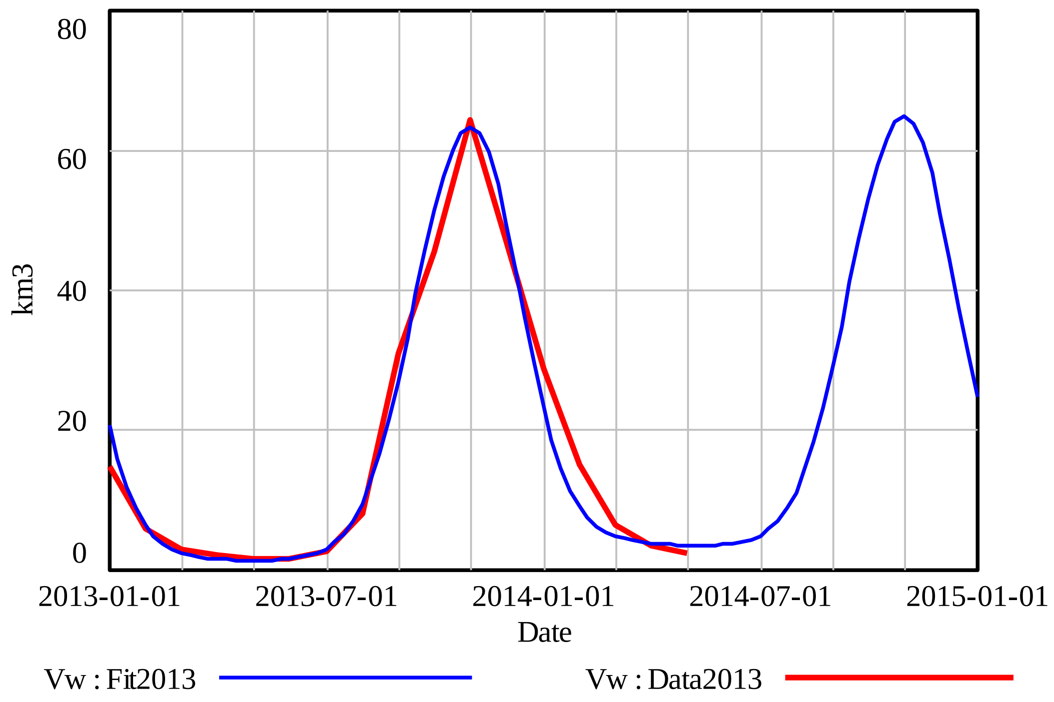

Figure 10: Calibrated seasonal water volume of the lake in 2013

4. Simulation results and discussion

Kummu and Sarkkula (2008) compiled a cumulative impact assessment of the construction for large-scale hydropower dams and reservoirs in the upper part of the Lower Mekong Basin. They based their assessment of the impact on the flow to TS Lake by reviewing reports of the Mekong River Commission (MRC) and the Asian Development Bank (ADB). The authors predicted that over a 20-year time frame with a high development scenario, the maximum water level of the lake will be lowered by 0.36 to 0.54m and the minimum water level of the lake would increase by as much as 0.6 m. The authors also predicted then that there would be a change in water discharge to the lake. Lauri et al (2012) also wrote that the simulated change in discharge at Kratie (Cambodia) between the baseline (1982–1992) and projected time period (2032–2042) ranges from −11% to +15% for the wet season and −10% to +13% for the dry season. While these studies provide rich quantitative information on the change of the discharge rate, it is not practical and useful to build a dynamic model of phosphorus taking into account all of these changes. Our approach was to build a reasonable simple dynamic model that can be tested again time series data available at different time (2001 and 2013). The hope was that the simple model would be capable of producing reasonably well the dynamic behavior of particulate and dissolved phosphorus.

The main variables of the model are particulate and dissolved phosphorus in the lake water column. While the model generated the behavior of the dissolved phosphorus of the lake reasonably well, the model failed to explain the peak of the particulate phosphorus in the lake in May despites many simulations with changing values of parameters of the model. **Figure 11** and **Figure 12** show predictions of the model together with actual PP and DP measurements in 2001 for comparison while **Figure 13** and **Figure 14** show the predictions of the model with actual PP and DP measurements in 2013. The model generated reasonably well behavior for DP and PP in water column in 2001 and particularly well for the behavior of PP in 2013. Unfortunately, the model did not work well to predict the DP in water column in 2013.

Limitations of the model and results can be linked to the modeling process and the data used to calibrate and provide predictions of nutrient conditions. The completely mixed system assumption used in the model in this paper may be violated in Tonle Sap Lake during the wet season when the lake is deep enough for thermal stratification. This could isolate much of the lake bottom from interactions with the surface layer. Also, there are limitations with the data used in the modeling process. This study assumed nutrient concentrations from the main river channel and tributaries to the TS Lake are the same while this is not known. However, the results are encouraging enough to merit further investigation.

Simulating PP in water column (PPw) in 2001

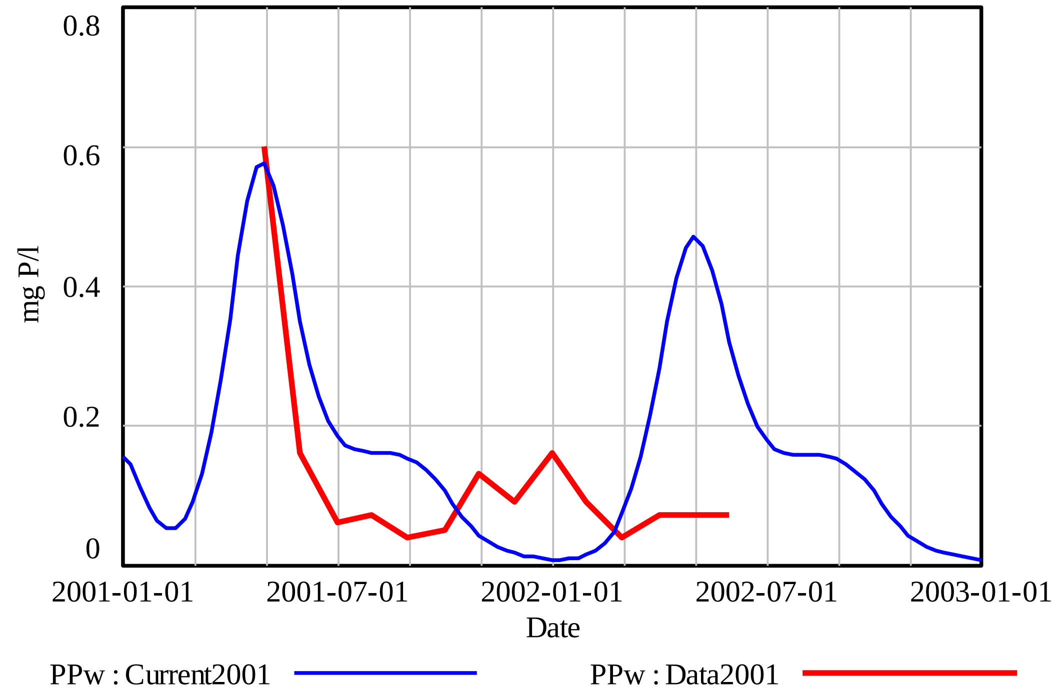

Figure 11: Simulated behavior of PPw in 2001

Simulating DP in water column in 2001

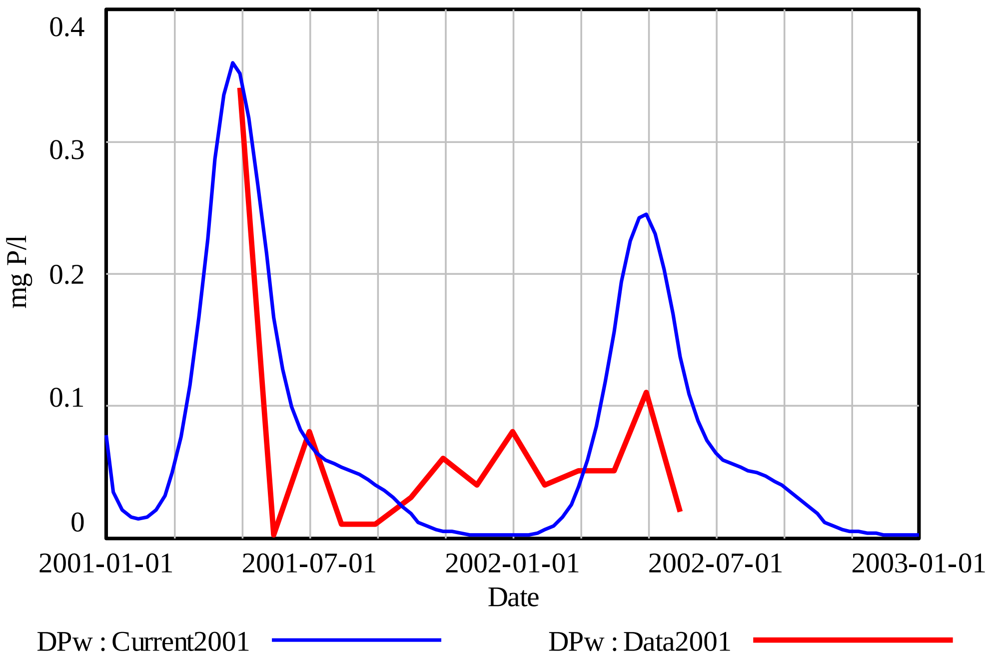

Figure 12: Simulated behavior of DPw in 2001

Simulating PP in water column in 2013

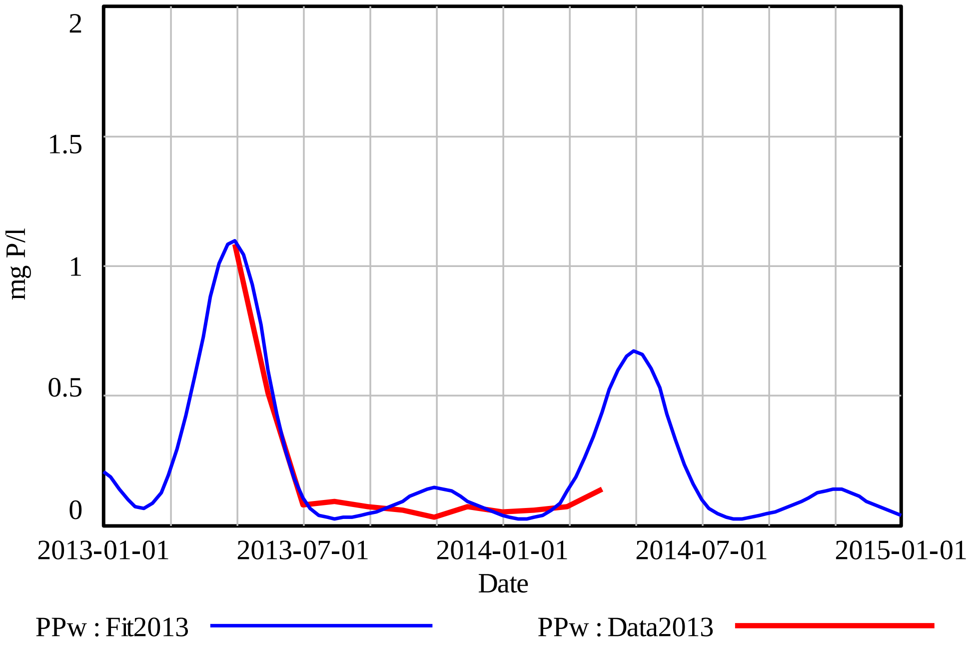

Figure 13: Simulated behavior of PPw in 2013

Simulating DP in water column in 2013

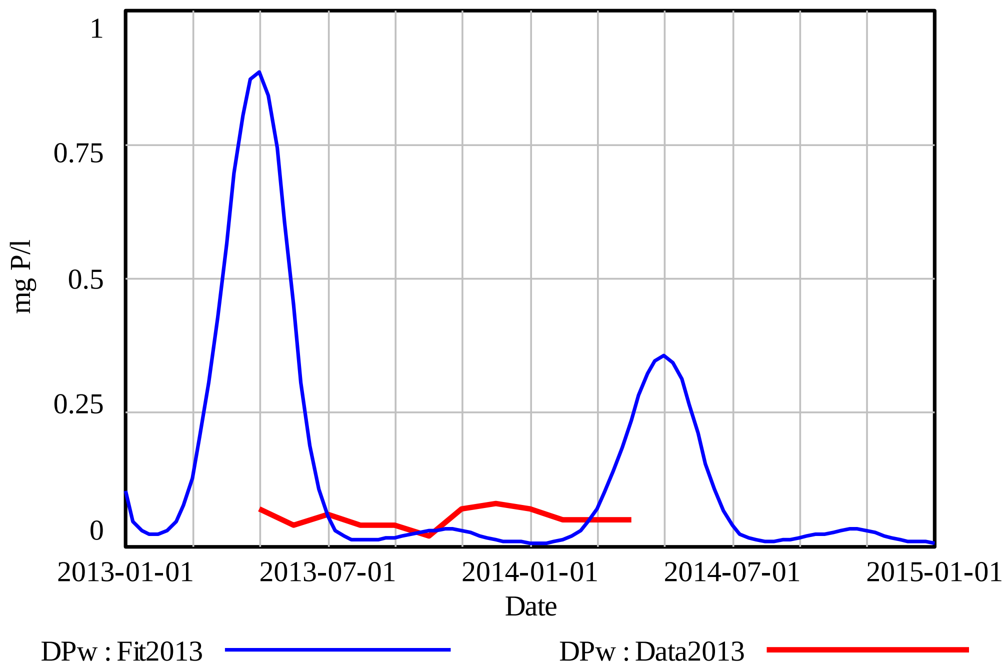

Figure 14: Simulated behavior of DPw in 2013

5. Conclusion

A relatively simple SD model has been shown to be capable of simulating DP and PP dynamic concentrations in Tonle Sap Lake. The calculated results are in generally in agreement with actual reported concentrations over a one-year period at different times (2001 and 2013). Some parameters like settling velocity and conversion rates from DP to PP and vice versa were not measured in this study. Rather, model constants were chosen via a calibration approach to agree with actual observations in 2001 and 2013 when we have available time-series data. Some have suggested that model calibration alone might not be adequate for validation and testing of phosphorus model mechanisms and independent measurements of model fluxes and coefficients should be performed in association with model development to reduce the overall model uncertainty (Seo & Canale, 1996). While this seems appealing to modelers in Environmental Engineering, we would argue that it is not always the case. In our study, many simulation runs have been performed during calibration of the SD model of P presented here and we found the model is not very sensitive to these parameters. So these parameters are not required for a very precise estimate. It should be noted that these parameters are not only very difficult to measure but the mechanisms underlying the processes are complicated and oftentimes poorly understood. This is the reason why we tried to justify the use of SD approach for modeling phosphorus dynamics in the lake as written in our research proposal submitted to APN.

Acknowledgement

We are greatly indebted to Matti Kummu, a research fellow at the Water and Development Research Group and Assistant Professor at Aalto University for helpful discussion and the sharing of the data. We are deeply indebted to the financial support for this project provided by the Asia-Pacific Network for Global Change Research (Award #ARCP2012-17NMY-Burnett).

References

Imboden, D. M. (1974). Phosphorus model of lake eutrophication. *Limnology and Oceanography, 19*((2): 297-304).

Kummu, M., & Sarkkula, J. (2008). Impact of the Mekong River flow alteration on the Tonle Sap flood pulse. *Ambio, 37(3): 185-192*.

Lung, W. S., Canale, R. P., & Freedman, P. L. (1976). Phosphorus models for eutrophic lakes. *Water Research, 10: 1101-1114*.

Snodgrass, W. J., & O'Melia, C. R. (1975). Predictve model for phosphorus in lakes. *Environmental Science & Technology, 9*(10): 937–944).

Vensim, Ventana Systems, Ver. 5. Harvard MA, USA, 2012

Lauri H., de Moel H., Ward P. J., Rasanen T. A., Keskinen M., and Kummu M. (2012). Future changes in Mekong River hydrology: impact of climate change and reservoir operation on discharge. *Hydrology and Earth System* Sciences, 16: 4603–4619.

Seo, D., & Canale, R. P. (1996). Performance, reliability and uncertainty of total phosphorus models for lakes—I. Deterministic analyses. Water Research, 30 (1): 83–94.

Basic equations of the model

****

(001) A= km2*1759.8*(Vw/UnitVol)^0.4889

Units: km2

****
(002) a0= 17.93
Units: km3/Month
Fitting constant
****
(003) a1= 1
Units: km3/Month
Fitting constant
****
(004) a2= 4.5e-006
Units: km3/Month
Fitting constant
****
(005) c0= -1.88
Units: km3/Month
Fitting constant
****
(006) c1= 1
Units: km3/Month
Fitting constant
****
(007) c2= 8e-006
Units: km3/Month
Fitting constant
****
(008) d0= 6.28
Units: Month
Fitting constant
****
(009) d1= 7.2
Units: Month
Fitting constant
****
(010) d2= 4.5
Units: Month
Fitting constant
****
(011) DiffuseFromGW= conv*DPinGW*GWflow
Units: Tonne/Month
****
(012) DiffuseFromSed= 5.5
Units: Tonne/Month
****
(013) DP=

INTEG (DiffuseFromGW+DiffuseFromSed+DPin+"RatePP-DP"-DPout-"RateDP-PP",

2152)

Units: Tonne

****

(014) DPin= conv*((DPinRiver*TS Inflow)+(DPinTr*"Tributaries.Flow"))

Units: Tonne/Month

****

(015) DPinGW= 0.14

Units: mg P/l

****

(016) DPinRiver= 0.35

Units: mg P/l

****

(017) DPinTr= 0.1

Units: mg P/l

****

(018) DPout= conv*DPw*Outflow

Units: Tonne/Month

****

(019) DPw= conv1*DP/Vw

Units: mg P/l

****

(020) EvapoRate= Vw*FractEvapoRate

Units: km3/Month

****

(021) FINAL TIME = 24

Units: Month

The final time for the simulation.

****

(022) FractEvapoRate= 0.06

Units: 1/Month

****

(023) GWflow=

(a2*sin(2*3.14159*(Time-d2)/period b2)+c2)*EXP(h2*cos(2*3.14159*(Time-d2)/period b2))+0.1

Units: km3/Month

****

(024) h0= 1.14

Units: Dmnl

Fitting constant

****

(025) h1= 2.61

Units: Dmnl

Fitting constant
****
(026) h2= 12
Units: Dmnl
Fitting constant
****
(027) Inflow= TributariesFlow+TS Inflow
Units: km3/Month
****
(028) INITIAL TIME = 0
Units: Month
The initial time for the simulation.
****
(029) Ks= 3.5
Units: m/Month
****
(030) mu1= 5
Units: 1/Month
****
(031) mu2= 0.5
Units: 1/Month
****
(032) Outflow= IF THEN ELSE(TS RiverFlow<0, -TS RiverFlow, 0)
Units: km3/Month
****
(033) period b= 12
Units: Month
****
(034) period b2= 12
Units: Month
****
(035) PP=
INTEG (PPin+"RateDP-PP"+ResuspendFromSed-PPout-"RatePP-DP"-Settling,
4304)
Units: Tonne
****
(036) PPin= conv*((PPinRiver*TS Inflow)+(PPinTr*"Tributaries.Flow"))
Units: Tonne/Month
****
(037) PPinRiver= 0.288
Units: mg P/l
****
(038) PPinTr= 0.3
Units: mg P/l

****
(039) PPout= conv*PPw*Outflow
Units: Tonne/Month
****
(040) PPw= conv1*PP/Vw
Units: mg P/l
****
(041) "RateDP-PP"= mu1*DP
Units: Tonne/Month
****
(042) "RatePP-DP"= PP*mu2
Units: Tonne/Month
****
(043) ResuspendFromSed= 20
Units: Tonne/Month
****
(044) Settling= coeff2*Ks*A*PP/Vw
Units: Tonne/Month
****
(045) "Tributaries.Flow"=
(a1 0*cos(2*3.14159*(Time-d1 0)/period b)+c1 0)*EXP(h1 0*sin(2*3.14159*(Time -d1 0)/period b))
Units: km3/Month
****
(046) TS Inflow= IF THEN ELSE(TS RiverFlow>=0, TS RiverFlow, 0)
Units: km3/Month
****
(047) TS RiverFlow=
(a0*cos(2*3.14159*(Time-d0)/period b)+c0)*EXP(h0*(sin(2*3.14159*(Time-d0) /period b)+k0))
Units: km3/Month
****
(048) Vw= INTEG (Inflow-EvapoRate-Outflow, 27.78)
Units: km3